

# Optical Excitations in Cold Gases

by

Mehmet Özgür Oktel

B.S. in Physics. Middle East Technical University. 1996,  
B.S. in Electrical Engineering. Middle East Technical University. 1996

Submitted to the Department of Physics  
in partial fulfillment of the requirements for the degree of

Doctor of Philosophy in Physics

at the

MASSACHUSETTS INSTITUTE OF TECHNOLOGY

February 2001

© Massachusetts Institute of Technology 2001. All rights reserved.

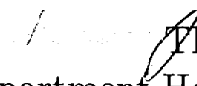
Author .....

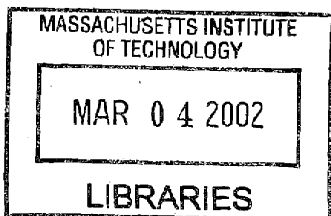
Department of Physics  
November 2, 2000

Certified by

.....  
Leonid S. Levitov  
Professor  
Thesis Supervisor

Accepted by .....

 Thomas J. Greytak  
Professor, Associate Department Head for Education



ARCHIVES

# Optical Excitations in Cold Gases

by

Mehmet Özgür Oktel

Submitted to the Department of Physics  
on November 2, 2000, in partial fulfillment of the  
requirements for the degree of  
Doctor of Philosophy in Physics

## Abstract

In this thesis, we study the effects of interparticle interactions on the optical spectrum of cold gases. We first consider homogenous gas in the weak excitation regime and find that the optical spectrum of a system of Bosons is highly sensitive to interactions. We find that optical excitations, at temperatures low enough for the thermal de Broglie wavelength to be larger than the scattering length, become collective modes. We study collective affects in the optical spectrum both above and below Bose-Einstein condensation, and show that the spectrum acquires a doublet structure when the condensate forms. We present a detailed theory of spectral shift and an estimate of some of the broadening effects.

We derive a sum rule for the average frequency shift of an optical spectrum and investigate the basic conservation laws and symmetries of the system lying at the basis of this sum rule. We also compare the sum rule for the optical spectrum with the f-sum rule for the density-density correlation function.

Finally we derive a transport equation for the optical modes in a dilute Bose system, which allows us to study the non-linear response to the excitation field. We map the problem onto the dynamics of two interacting anisotropic spins, and calculate the precession frequencies exactly both below and above Bose condensation. We demonstrate a relation between Rabi oscillations and internal Josephson oscillations, and find that an analogue of the internal Josephson effect exists in a non-condensed system. We also derive the transport equation for a dilute Fermi system and find that the dependence of the precession frequencies on interparticle interactions is very weak for fermions.

Thesis Supervisor: Leonid S. Levitov

Title: Professor

## Acknowledgments

I would like to express my deepest gratitude to my supervisor Leonya Levitov. Without his expert guidance this thesis would not have been possible. He explained when I asked, helped when I struggled and was patient when I failed. I admire his creativity and thank him for a graduate study which never got boring.

I am also grateful to Prof. Kleppner and Prof. Greytak for their help. I have benefited from many useful discussions with them, and their students Tom Killian, Lorenz Willmann, Stephen Moss and David Landhuis. Tom has explained many details of the experiments to me and it was his questions which led us to consider some of the topics explored in this thesis.

I have taken some wonderful courses throughout my Ph.D. Most notably, quantum mechanics classes of Prof. Negele, statistical mechanics classes of Prof. Berker and Prof. Kardar, quantum field theory classes of Prof. Coleman and atomic physics classes of Prof. Ketterle were vital to my progress.

If you start a casual conversation with anyone in the condensed matter theory corridor here, chances are you are going to learn something interesting about physics. I have tried this many times and probably have learned as much physics from the people around here as I have learned from the courses. Apart from “intellectual” conversations, I have also shared many laughs with Alkan Kabakçioğlu, Anna Lopatnikova, Tairan Wang, Sohrab Ismail-Beigi, Dicle Yeşilleten, Gabriela Migliorini, Joshua Weitz, Joel Moore, Adam Durst, Walter Rantner, Zoran Hadjibabic, Jens Siewert, Martin Kunz, Darren Segall, Torkel Engness, Dima Novikov, Maksim Skrobogatiy, Sasha Abanov, Rava daSilveira, Mehdi Yahyanejad, Michelle Povinelli, Evan Reed, Shanhui Fan and Sven Heemayer.

I should also thank my friends in the Boston area for all the fun we had here over the last four years, Orhan Karşılığ and Ozan Kandamar were excellent roommates and will remain lifelong friends; Gökhan and Yasemin Güneş have listened to me complain about life many times; Asuman and Emre Köksal were always fun to talk to; and Oguz and Burcu Güneş have helped me a lot in my first year. Erdem and

Yasemin Erten have shared many bottles of *Raki* along with excellent *meze* with me. I regret that I got to know them so late especially after discovering that Erdem is as much a soccer fan as I am. On that note, I also thank Galatasaray soccer team for the last four excellent years, their success makes me happy even when I can not watch their games.

Alkan and Dicle deserve another round of thanks for providing me the opportunity to discuss physics in Turkish and for their friendship. Dicle has also given my thesis a thorough reading and made lots of useful suggestions.

Some of my friends, although thousands of miles away, were always with me thru their e-mails and phone calls. I thank Mithat Ünsal, Arkadaş Özakın, Altug Özpineci, Emrah Kalemci and Ayca Kumluca for their friendship and support.

Finally I would like to thank my parents for their love, encouragement and support. Even when facing very tough times, they have never failed to set excellent examples for me, with their dedication to each other, enthusiasm for their work and sincere piety. This thesis is dedicated to them.

# Contents

<b>1</b>	<b>Introduction</b>	<b>9</b>
1.1	Motivation . . . . .	9
1.2	Length Scales . . . . .	10
1.3	Overview . . . . .	13
<b>2</b>	<b>Optical Excitations in a Non-Ideal Bose Gas</b>	<b>15</b>
2.1	The Hamiltonian . . . . .	15
2.2	Kubo formula for Optical Excitations . . . . .	17
<b>3</b>	<b>Calculation of the Optical Spectrum</b>	<b>20</b>
3.1	Optical Spectrum Above Bose-Einstein Condensation . . . . .	20
3.2	Predictions for the Spectrum . . . . .	29
3.2.1	The dispersion relation . . . . .	29
3.2.2	Broadening . . . . .	32
3.3	Optical Spectrum Below Bose-Einstein Condensation . . . . .	35
<b>4</b>	<b>Collective Properties of Optical Excitations</b>	<b>43</b>
4.1	Transport Equation . . . . .	47
<b>5</b>	<b>A Sum Rule for the Cold Collision Frequency Shift</b>	<b>61</b>
<b>6</b>	<b>Nonlinear Optical Response</b>	<b>68</b>
6.1	The Single Spin Problem . . . . .	72
6.2	The Two Spin Problem . . . . .	79

6.3 Fermions . . . . .	85
<b>7 Conclusion</b>	<b>90</b>

# List of Figures

3-1	Various diagrams used in the calculation of the normal gas response.	26
3-2	Diagrammatic representation of the ladder series approximation.	27
3-3	Absorption spectrum above BEC at fixed temperature and varying density: $n = fn_{\text{BEC}}$ , $0.5 \leq f < 1$ . The frequency shift $\Delta\omega$ is defined relative to the that of a free atom at rest: $\Delta\omega = \omega - \omega_0 - k^2/2m$ . Spectral power $\mathcal{I}$ is normalized by particle density $n$ . The excitation wavevector $k$ is 0.5 in the units of $\lambda_{12}n_{\text{BEC}}/v_T$ . The interaction constant $\lambda_{11}$ is chosen to be 0. Note that the peak position follows the relation (3.40).	30
3-4	Various diagrams used in the calculation of the condensate response.	37
3-5	Absorption spectrum in the BEC regime, shown for temperature varying between 0 and $T_c$ ; density $n$ fixed. The excitation wavevector $k$ is $2/3$ in the units of $\lambda_{12}n/v_T$ . Lines in the base plane indicate the peak positions for $k = 0$ (3.56). Note narrowing of the spectral line with decreasing $T$ , and strengthening of the condensate peak due to increasing condensate fraction. (The frequency shift $\Delta\omega$ is defined in Fig.3-3; $\lambda_{11} = 0$ .)	40
3-6	Absorption spectrum in the BEC regime at fixed temperature and density varying from $n_{\text{BEC}}$ and up. Excitation wavevector $k = 2.5$ in the units of $\lambda_{12}n_{\text{BEC}}/v_T$ . Increasing condensate density leads to narrowing of the peaks and to strengthening of the condensate peak, as in Fig.3-3. ( $\Delta\omega$ and $\mathcal{I}$ are defined in Fig.3-3; $\lambda_{11} = 0$ .)	41





# Chapter 1

## Introduction

### 1.1 Motivation

This thesis is written at a time when the recent experimental demonstration of Bose–Einstein condensation in dilute gases has caused great excitement in both the experimental and theoretical communities. Two branches of physics, condensed matter physics and atomic physics which developed mostly independently over the last four or five decades, have joined together in an attempt to understand this new state of matter. Although Bose–Einstein condensation (BEC) of atoms has previously been observed in superfluid  $^4\text{He}$ , the new experiments have led to a wide variety of new inquiries into the nature of BEC in dilute systems.

The first experiments that realized BEC in dilute atomic gases were carried out with alkali gases, Rb, Na and Li [4, 12, 9, 10]. A common feature of all these experiments was that they used one form of real space imaging, either reconstruction from time of flight data, or imaging by light scattering, to observe the formation of the condensate. Following these experiments, in 1998, the MIT spin polarized hydrogen group succeeded in getting Hydrogen atoms to form a BEC [14]. Apart from fulfilling the twenty year goal of getting a Hydrogen condensate, this was the first case in which the condensate was probed by optical spectroscopy [24]. This experiment posed a number of interesting questions about the optical properties of a dilute gas at very low temperatures.

The spectrum obtained in the MIT Hydrogen BEC experiment was the starting point for this thesis. However, the reader should realize that, although at times we will make connection to this experiment and point out the consequences of some of our results regarding other experiments, the main set of issues that we address is more along the basic theory lines. In particular, we are concerned with the following general questions: In a dilute system, how are the optical excitations, excitations involving the change of the internal state of constituent particles, affected by interparticle interactions? And what is the manifestation of exchange and quantum statistics effects?

In trying to answer these questions, we will consider systems both above and below BEC transition. As well as investigating the weak excitation limit, in which the number of particles changing their internal state is negligible compared to the total number of particles, we will also consider systems in which a large fraction of the atoms undergo the internal state transition. One reason for the latter consideration is that, unlike in conventional condensed matter systems, such experiments are routinely performed on dilute gases in studying BEC [19, 18]. Another reason is that the novel exchange effects that we describe below become quite interesting in this non-linear regime.

## 1.2 Length Scales

We shall see that understanding the effects of interparticle interactions on the optical spectrum of a cold gas constitutes a quantum many body problem. However, before using tools of quantum theory to attack the problem, one has to justify that this sophisticated approach is indeed needed. After all, we are concerned with the properties of a dilute gas: the experiments we are interested in are actually done on systems which are five orders of magnitude less dense than air [23]. The study of weakly interacting dilute gases at high temperatures has been completed by the successful use of classical mechanics a long time ago. Such systems have even taken their place as examples in statistical mechanics textbooks [28]. Why would then anyone want to

use anything more complicated than classical mechanics to understand a dilute gas.

The answer to this question can be seen from analyzing the length scales in an interacting dilute system. The density of the system,  $n$ , gives us the first length scale,  $n^{-1/3}$ , which is the mean interparticle distance. The interparticle interactions are characterized by the scattering cross section,  $\sigma$ , which defines an interaction length scale via the effective scattering length,  $a \sim \sqrt{\sigma/4\pi}$ . The system is considered dilute when the interaction range is much smaller than the average interparticle separation

$$n^{-1/3} \gg a. \quad (1.1)$$

Another length scale to be taken into account characterizes the extent of quantum mechanical behavior shown by the constituent particles. This length scale is the extent of the wavepacket of a particle moving with average thermal velocity,  $v_T = \sqrt{\frac{2k_B T}{m}}$ . Comparing the thermal de Broglie wavelength

$$\lambda_T \sim \frac{\hbar}{mv_T} \quad (1.2)$$

with other length scales allows one to evaluate the importance of quantum mechanics in the problem. As long as the temperature is high enough so that the thermal de Broglie wavelength is much less than the two other length scales,  $n^{-1/3} \gg a \gg \lambda_T$ , we can ignore quantum mechanics and use classical statistical mechanics to understand the effects of interactions. However, there are two other less trivial regimes.

The first possibility is that the temperature is low enough, so that the thermal de Broglie wavelength is larger than the scattering length, but high enough for the interparticle separation to remain as the largest length scale:

$$n^{-1/3} \gg \lambda_T \gg a. \quad (1.3)$$

In this case the statistical properties of the atoms can still be thought as classical, however, the collisions have already become quantum mechanical. The first consequence of this is that we only need to consider the s-wave scattering between the particles

[27, 49]. Thus, the interactions are now characterized by the s-wave scattering length,  $a_s$ , while scattering in all higher angular momentum channels are suppressed.

Another more subtle consequence is that the effects of interparticle interactions on the quantum mechanical phase of the particle's wavefunction become important in the regime given in (1.3) [43, 44, 7]. To explain that we note that the phase coherence is destroyed every time the particle undergoes a collision. During the time interval between the collisions,

$$\tau_{\text{free}} \sim (4\pi a^2 n v_{\text{T}})^{-1}, \quad (1.4)$$

the particles move in the interaction potential of all the other particles. After averaging the interparticle interaction over the path of a single particle, we get the effective potential energy due to interactions

$$V = \frac{4\pi \hbar^2 a_s}{m} n. \quad (1.5)$$

Thus, compared to a free particle, during the time  $\tau_{\text{free}}$  the particle accumulates an extra quantum phase of

$$\phi = \frac{V \tau_{\text{free}}}{\hbar} \simeq \lambda_{\text{T}}/a_s. \quad (1.6)$$

When the phase  $\phi$  is much larger than  $2\pi$ , quantum mechanical effects are quite important. In particular in the regime (1.3) certain collective effects can exist in a dilute gas. Another way to picture it would be to say that in collisions the scattering length  $a_s$ , is replaced by  $\lambda_{\text{T}}$ , increasing the effective cross sections, and thus the importance of interactions in the system. The gas in this regime has been named a *quantum gas*, and some of the properties, especially the physics of spin waves in these systems, have been investigated by Bashkin, Lhuiller and Laloe, and Levy and Ruckenstein [7, 32, 33, 31]. We will use methods of quantum many-body theory to investigate the optical excitations of a quantum gas.

The second regime we will consider is that of very low temperatures, such that

the thermal de Broglie wavelength,  $\lambda_T$ , is the largest length scale at hand,

$$\lambda_T \gg n^{-1/3} \gg a. \tag{1.7}$$

When  $\lambda_T$  becomes larger than the interparticle separation, wavefunctions of particles in the gas start to overlap. This overlap, combined with the Bosonic tendency to be in the same quantum state, leads to Bose–Einstein condensation [29]. In a Bose condensed system, a finite fraction of the particles share the same wavefunction, forming the condensate, while the rest of the particles are distributed over the energies above the condensate.

To summarize the discussion, in both regimes of (1.3) and (1.7), physical properties of interest are essentially quantum mechanical. Therefore in order to address interactions in these regimes we shall employ the methods of quantum many body theory.

### 1.3 Overview

This thesis is organized as follows: in Chapter 2 we introduce the Hamiltonian and derive an expression for the lineshape of optical excitations in a uniform system. In chapter 3 we use diagrammatic perturbation theory to evaluate the lineshape above and below BEC. After that we discuss predictions for line shifts, broadening, and the overall structure of the spectrum. In chapter 4 a transport equation is derived for the collective optical excitations, which, together with the results of chapter 3, will be used to discuss the physics underlying the collective effects seen in the lineshape.

In chapter 5 we derive a general sum rule for the mean frequency shift in the optical spectrum resulting from interactions. We discuss the conservation rules and symmetries that form the physical basis for the sum rule. Finally we compare this sum rule to the f-sum rule for density excitations.

Chapter 6 is devoted to the study of strong optical excitations, in which a significant fraction of particles change their internal state. We make predictions for

experiments using atomic clocks, and also compare the nature of optical excitations in Fermi and Bose gases. Finally in chapter 7 we summarize our results and their connection to experiments.

# Chapter 2

## Optical Excitations in a Non-Ideal Bose Gas

### 2.1 The Hamiltonian

We start our study of optical excitations by defining a model that incorporates the basic physics of a dilute gas with two internal states. Throughout this chapter, we are going to consider a dilute gas of uniform density. Each of the particles in the gas can be in one of the two internal states, state 1 or state 2, the energy separation of these two states being  $\hbar\omega_0$ , and we further assume that the dispersion relation for free particles does not depend on the internal state they are in.

In general, two atoms in the gas will interact via some potential  $V(r)$ , which depends on the internal states of the atoms. Analysis of the scattering problem is simplified by realizing that at low temperatures such that the wavelength  $\lambda_T$  is greater than the interaction radius, only s-wave scattering is important [20]. In this regime the potential  $V(r)$  can be replaced by a pseudopotential:

$$V(r) = \lambda\delta(r). \tag{2.1}$$

The interaction parameter  $\lambda$  is related to the s-wave scattering length as:

$$\lambda = \frac{4\pi\hbar^2 a_s}{m}. \quad (2.2)$$

The scattering length  $a_s$  depends on the internal states of the scattering particles. In a problem with two internal states, we have three different scattering lengths, and thus three interaction parameters. We will call the s-wave scattering length for scattering of two particles in state 1 (state 2),  $a_{11}$  ( $a_{22}$ ). Scattering length for a collision involving one particle in state 1 and one in state 2 will be  $a_{12}$ , which can also be written as  $a_{21}$ . The interaction parameters,  $\lambda_{11}$ ,  $\lambda_{12}$  and  $\lambda_{22}$  are related to the corresponding scattering lengths as in Eq.(2.2).

Within these approximations, the system is described by second quantized Hamiltonian  $\mathcal{H} = \mathcal{H}_0 + \mathcal{H}_1$ , where

$$\mathcal{H}_0 = \sum_p \frac{p^2}{2m} a_p^\dagger a_p + \sum_p \left( \frac{p^2}{2m} + \omega_0 \right) b_p^\dagger b_p, \quad (2.3)$$

$$\begin{aligned} \mathcal{H}_1 &= \frac{1}{2} \sum_{p_1, p_2, q} \left( \lambda_{11} a_{p_1}^\dagger a_{p_2}^\dagger a_{p_2-q} a_{p_1+q} + \lambda_{22} b_{p_1}^\dagger b_{p_2}^\dagger b_{p_2-q} b_{p_1+q} \right) \\ &+ \lambda_{12} \sum_{p_1, p_2, q} a_{p_1}^\dagger a_{p_1+q} b_{p_2}^\dagger b_{p_2-q}. \end{aligned} \quad (2.4)$$

Here the annihilation operator  $a_p$  ( $b_p$ ) annihilates a particle in internal state 1 (2), occupying the translational state with momentum  $p$ . The operators  $a_p$ ,  $b_p$  satisfy the canonical Bosonic commutation relations,

$$[a_p, a_{p'}^\dagger] = \delta_{p, p'}; \quad [a_p, a_{p'}] = 0; \quad [a_p^\dagger, a_{p'}^\dagger] = 0, \quad (2.5)$$

$$[b_p, b_{p'}^\dagger] = \delta_{p, p'}; \quad [b_p, b_{p'}] = 0; \quad [b_p^\dagger, b_{p'}^\dagger] = 0. \quad (2.6)$$

Also, any operator of type a commutes with any operator of type b.

The Hamiltonian in this form conserves the number of particles in internal states 1 and 2 separately. We will assume that optical excitations, which involve transitions from state 1 to state 2, are stimulated by an external classical field. This assumption



gives one more term to be added to the Hamiltonian,  $\mathcal{H} = \mathcal{H}_0 + \mathcal{H}_1 + \mathcal{H}_{exc}$ , with

$$\mathcal{H}_{exc} = \sum_{p,k} A_k e^{-i\omega t} b_{p+k}^+ a_p + h.c. \quad (2.7)$$

where  $A_k$  are the external field harmonics

$$A_k = \int d^3r e^{i\vec{k}\cdot\vec{r}} A(r). \quad (2.8)$$

In this chapter we will consider the case of weak external field, so that the total number of particles that are optically excited is negligible compared to the total number of particles. This assumption will be relaxed in chapter 6 where we study the problem of strong excitation.

## 2.2 Kubo formula for Optical Excitations

The Hamiltonian introduced in the previous section in Eq.(2.4,2.5,2.7) describes the dilute system in the presence of an external field which causes internal state transitions. The aim of this section will be to get a general expression for the optical spectrum starting from the Hamiltonian.

The optical spectrum of the sample is measured by exposing it to a weak external field, as in Eq.(2.7), and then counting the number of particles changing their internal states, per unit time at steady state. Equivalently, this is also the number of field quanta absorbed per unit time, *i.e.*, the optical response of the medium. The optical spectrum is obtained by measuring how this response varies as a function of the frequency  $\omega$  of the external field.

We are thus interested in calculating the transition rate,

$$\left\langle \frac{d\hat{N}_2(t)}{dt} \right\rangle, \quad \hat{N}_2 = \sum_p b_p^+ b_p, \quad (2.9)$$

as a function of  $k$  and  $\omega$  of the field  $A(k, \omega)$ . The average is calculated in the grand

canonical ensemble,

$$\left\langle \frac{d\hat{N}_2(t)}{dt} \right\rangle = \text{Tr} \left\{ \frac{d\hat{N}_2(t)}{dt} \hat{\rho} \right\} = \sum_m \langle m | \frac{d\hat{N}_2(t)}{dt} \hat{\rho} | m \rangle, \quad (2.10)$$

where the trace is carried out over all the many-particle eigenstates, indexed by  $m$ . The density matrix  $\hat{\rho}$  is defined as usual,

$$\begin{aligned} \hat{\rho} &= \mathcal{Z}^{-1} \sum_m e^{-\epsilon_m/T} |m\rangle \langle m|, \\ \mathcal{Z} &= \sum_m e^{-\epsilon_m/T}, \end{aligned} \quad (2.11)$$

where  $\epsilon_m$  are the energies of the many particle eigenstates  $|m\rangle$ .

We begin the calculation by writing the Heisenberg equation of motion for  $\hat{N}_2$

$$\begin{aligned} \frac{d\hat{N}_2}{dt} &= i[\mathcal{H}(t), \sum_p b_p^+ b_p] \\ &= i[\mathcal{H}_{exc}, \sum_p b_p^+ b_p] \\ &= ie^{i\omega t} \sum_{p,k} A_k b_{p+k}^+ a_p - ie^{-i\omega t} \sum_{p,k} A_k^* a_p^+ b_{p+k} \\ &= ie^{i\omega t} \hat{C} - ie^{-i\omega t} \hat{C}^+. \end{aligned} \quad (2.12)$$

Here we defined

$$\hat{C} = \sum_{p,k} A_k^* \hat{\eta}_{p,k}, \quad \hat{\eta}_{p,k} = a_p^+ b_{p+k}. \quad (2.13)$$

We can now rewrite  $\mathcal{H}_{exc}$  as

$$\mathcal{H}_{exc} = e^{i\omega t} \hat{C} + e^{-i\omega t} \hat{C}^+, \quad (2.14)$$

and obtain

$$\left\langle \frac{d\hat{N}_2(t)}{dt} \right\rangle = \text{Tr} \left\{ (ie^{i\omega t} \hat{C} - ie^{-i\omega t} \hat{C}^+) \hat{\rho}(t) \right\}. \quad (2.15)$$

Here the time evolution of the density matrix is

$$\hat{\rho}(t) = \left[ \mathcal{T} e^{-i \int_0^t dt' \mathcal{H}(t')} \right] \hat{\rho}(0) \left[ \tilde{\mathcal{T}} e^{i \int_0^t dt' \mathcal{H}(t')} \right], \quad (2.16)$$

with  $\mathcal{T}$  and  $\tilde{\mathcal{T}}$  being the time ordering and reverse time ordering operators.

The next step is to make use of the assumption small of excitation field, by expanding the time evolution of the density matrix of Eq.(2.16) in powers of  $\mathcal{H}_{exc}$ . We will consider only the first order terms.

This is justified because in the zeroth order in the excitation field, we only have the sum of  $\mathcal{H}_0$  and  $\mathcal{H}_1$  as our Hamiltonian. Both of them conserve the number of particles in each internal state, hence to zeroth order we have no contribution to  $d\hat{N}_2/dt$ . We calculate the first order contribution to time evolution of  $\hat{\rho}$  by first going to an interaction representation with respect to  $\mathcal{H}_{exc}$  and then expanding the exponent. This gives

$$\hat{\rho}^{(1)}(t) = -i \int_{-\infty}^t dt' e^{-i(\mathcal{H}_0+\mathcal{H}_1)(t-t')} [\mathcal{H}_{exc}(t'), \hat{\rho}^{(0)}] e^{i(\mathcal{H}_0+\mathcal{H}_1)(t-t')}. \quad (2.17)$$

Finally, we have

$$\left\langle \frac{d\hat{N}_2(t)}{dt} \right\rangle = -i \text{Tr} \left\{ \int_{-\infty}^t dt' \frac{d\hat{N}_2(t)}{dt} e^{-i(\mathcal{H}_0+\mathcal{H}_1)(t-t')} [\mathcal{H}_{exc}(t'), \hat{\rho}^{(0)}] e^{i(\mathcal{H}_0+\mathcal{H}_1)(t-t')} \right\}. \quad (2.18)$$

By using the cyclic property of the trace and the expressions Eq.(2.13),(2.14) we obtain the response function of  $d\hat{N}_2/dt$  to the excitation field  $A(k, \omega)$ . The imaginary part of this response function gives the optical spectrum of the system [1],

$$\begin{aligned} \mathcal{I}(\omega) &= \text{Im} \left\{ \int_0^{\infty} e^{i\omega t} \text{Tr} \{ [e^{i(\mathcal{H}_0+\mathcal{H}_1)t} \hat{C}^+ e^{i(\mathcal{H}_0+\mathcal{H}_1)t}, \hat{C}] \hat{\rho} \} \right\} \\ &= \text{Im} \left\{ \int_0^{\infty} e^{i\omega t} \langle [\hat{C}(t), \hat{C}^+(0)] \rangle \right\}. \end{aligned} \quad (2.19)$$

This general formula allows one to calculate the optical spectrum starting from the microscopic Hamiltonian. As might have been expected, Eq.(2.20) has the familiar Kubo form [35, 26], encountered for all linear response calculations.

## Chapter 3

# Calculation of the Optical Spectrum

### 3.1 Optical Spectrum Above Bose-Einstein Condensation

In this section we evaluate the expression (2.20) for the absorption spectrum. The particle density in our system is low, and thus, it is natural to employ perturbation theory in the interparticle interaction (2.5), since this expression is quadratic in density. However, as we shall see, the calculation does not reduce to evaluating the lowest order contribution in the interaction. Instead, it is necessary to perform a resummation of the perturbation series to account for the interaction in the final state of the excitation.

We carry out the perturbation expansion using finite temperature Green's functions [1]. Consider the finite temperature response function:

$$\Pi(k, \tau) = -\langle T_\tau \{ \sum_{p_1} \hat{\eta}_{p_1, k}(\tau_1) \sum_{p_2} \hat{\eta}_{p_2, k}(\tau_2) \} \rangle, \quad (3.1)$$

with

$$0 < \tau_{1,2} < 1/T, \quad \tau = \tau_1 - \tau_2, \quad (3.2)$$

and  $T_\tau$  is the “time ordering” operator in imaginary time  $\tau$ . The finite temperature operators are linked to the operators in the Shrödinger representation as follows

$$\begin{aligned}\hat{\eta}_{p,k}(\tau) &= e^{H\tau}\hat{\eta}_{p,k}e^{-H\tau}, \\ \hat{\bar{\eta}}_{p,k}(\tau) &= e^{H\tau}\hat{\eta}_{p,k}^+e^{-H\tau}, \\ 0 < \tau < 1/T,\end{aligned}\tag{3.3}$$

where  $H$  is the full Hamiltonian of Eq.(2.4,2.5,2.7).

The optical spectrum Eq.(2.20) is related to the response function  $\Pi$  by analytic continuation from the upper complex plane as [35],

$$\mathcal{I}(\omega) = \text{Im}\left\{\sum_k |A_k|^2 \lim_{i\omega \rightarrow \omega+i\delta} \Pi(k, i\omega)\right\}.\tag{3.4}$$

We construct a perturbation theory, where our response function will be expressed in terms of the non-interacting temperature Green’s functions for the particles in states 1 and 2,

$$\begin{aligned}\mathcal{G}_I^0(k, \tau) &= \langle T_\tau a_k(\tau_1) \bar{a}_k(\tau_2) \rangle, \\ \mathcal{G}_{II}^0(k, \tau) &= \langle T_\tau b_k(\tau_1) \bar{b}_k(\tau_2) \rangle, \\ 0 < \tau < 1/T,\end{aligned}\tag{3.5}$$

where the operators  $a(\tau)$ ,  $b(\tau)$  are related to the corresponding Shrödinger operators:

$$a(\tau) = e^{H'\tau} a e^{-H'\tau}, \quad \bar{a}(\tau) = e^{H'\tau} a^+ e^{-H'\tau}, \quad 0 < \tau < 1/T,\tag{3.6}$$

where  $H'$  is the Hamiltonian without the interaction term. The diagrammatic representation of these functions is given in Fig.(3-1 a,b).

The Green’s functions (3.5) in diagrammatic perturbation theory will be joined together by interaction and external field vertices. As discussed above, there are three different interactions  $\lambda_{11}$ ,  $\lambda_{12}$ ,  $\lambda_{22}$ , which, for convenience, will be represented graphically by the same symbol (See Fig.(3-1 c,d,e). In the calculation of the response

function, we also have two vertices for the external field (See Fig.(3-1 f). The response function  $\Pi(k, \omega)$  is given by the sum of all possible connected diagrams that can be constructed between two external field vertices using the free Green's functions and the interaction vertices [36].

As a first step, we calculate the lineshape for the ideal non-interacting gas. We call the response function in this limit  $\Pi_0(k, \omega)$ . There is only one diagram to calculate (see Fig.(3-2) a). We have

$$\begin{aligned}
\Pi_0(k, \omega_n) &= T \sum_{\omega'_n} \int \frac{d^3p}{(2\pi\hbar)^3} \mathcal{G}_I^0(p, \omega'_n) \mathcal{G}_{II}^0(k+p, \omega_n + \omega'_n) \\
&= \int \frac{d^3p}{(2\pi\hbar)^3} \frac{n_B(\epsilon^I(p+k)) - n_B(\epsilon^{II}(p))}{i\omega_n - (\epsilon^I(p+k) - \epsilon^{II}(p))} \\
&= - \int \frac{d^3p}{(2\pi\hbar)^3} \frac{n_B(p^2/2m)}{(i\omega_n - \omega_0) - ((p+k)^2 - p^2)/2m}.
\end{aligned} \tag{3.7}$$

Here  $\epsilon^I, \epsilon^{II}$  are the dispersion relations for particles in states 1 and 2,

$$\epsilon^I(p) = p^2/2m, \quad \epsilon^{II}(p) = p^2/2m + \hbar\omega_0, \tag{3.8}$$

and  $n_B$  is the Bose distribution.

The optical spectrum obtained from this result using Eq.(3.4) is a Doppler broadened peak centered at  $\omega = \omega_0 + k^2/2m$ . For a spatially uniform excitation field one has to set  $k = 0$ . In this case there is no Doppler broadening:

$$\Pi_0(k=0, \omega_n) = -\frac{n}{i\omega_n - \omega_0} \Rightarrow \mathcal{I}(\omega) \propto \delta(\omega - \omega_0). \tag{3.9}$$

As a next step, we introduce the interactions. In the presence of the interactions, one has to sum an infinite number of diagrams to calculate the optical spectrum exactly. All these diagrams can be schematically summarized in the “skeleton diagram” of Fig.(3-2 b). Here the thick lines correspond to the full Green's functions for particles in state 1 and state 2. The triangle is the vertex part, which is the sum of all possible connected graphs linking an external field vertex to two Green's functions, one for state 1 particles, the other for state 2. We calculate both the full Green's

functions and the vertex part in a self-consistent approximation.

As the first step of our approximation, we start with the non-interacting Green's functions  $\mathcal{G}^0$ , and dress them with the self-energy parts. At low density it is suitable to use the self-energy parts which are first order in the interaction (see Fig.(3-1 g,h,i).

The two diagrams forming the self-energy for the first Green's function are called the direct (Hartree) Fig.(3-1 h) and exchange (Fock) Fig.(3-1 i) contributions. For a system of bosons with contact interaction, these contributions are equal and not dependent on energy or wavevector. For the Green's function of particles in state 1, the self-energy is

$$\Sigma_I = \Sigma_{direct} + \Sigma_{exchange} = 2\lambda_{11}n, \quad (3.10)$$

Whereas for the particles in state 2 there is only direct (Hartree) contribution Fig.(3-1 i):

$$\Sigma_{II} = \lambda_{12}n. \quad (3.11)$$

Thus the full greens functions take the form

$$\begin{aligned} \mathcal{G}_I(k, \omega_n) &= \frac{n(k)}{i\omega_n - p^2/(2m) - 2\lambda_{11}n} \\ \mathcal{G}_{II}(k, \omega_n) &= \frac{1}{i\omega_n - \omega_0 - p^2/(2m) - \lambda_{12}n}. \end{aligned} \quad (3.12)$$

We now consider the vertex part  $\Gamma$ . The zeroth order term in the interaction is simply  $\Gamma = 1$ . Similar to the approximation for the Green's functions, we define a "two particle self-energy" block, and add up an infinite series of blocks corresponding to the ladder series in Fig.(3-2 b). Due to the contact nature of the interaction, each of the blocks can be calculated independently, and will give the same result. We define

$$\Pi'_0(k, \omega_n) = T \sum_{\omega'_n} \int \frac{d^3p}{(2\pi\hbar)^3} \mathcal{G}_I(k+p, \omega_n + \omega'_n) \mathcal{G}_{II}(p, \omega'_n). \quad (3.13)$$

Then the vertex part will be given by the ladder diagrams, which are summed up as

a geometric series

$$\begin{aligned}\Gamma(k, \omega_n) &= 1 + \lambda_{12}\Pi'_0 + \lambda_{12}^2(\Pi'_0)^2 + \dots \\ &= \frac{1}{1 - \lambda_{12}\Pi'_0(k, \omega_n)}.\end{aligned}\tag{3.14}$$

In the ladder approximation, our response function is

$$\begin{aligned}\Pi &= \Gamma\Pi'_0 \\ &= \frac{\Pi'_0(k, \omega)}{1 - \lambda_{12}\Pi'_0(k, \omega)}.\end{aligned}\tag{3.15}$$

To understand this result (3.15) We first set  $k = 0$  to see how the interactions effect the response to a uniform external field. The calculation of  $\Pi'_0(k = 0, \omega)$  is the same as  $\Pi_0(k = 0, \omega)$ , resulting in

$$\Pi'_0(k = 0, \omega_n) = \frac{n}{i\omega_n - \omega_0 - \lambda_{12}n + 2\lambda_{11}n}.\tag{3.16}$$

Substituting (3.16) into Eq.(3.15), we obtain

$$\begin{aligned}\Pi(k = 0, \omega_n) &= \frac{\frac{n}{i\omega_n - \omega_0 - \lambda_{12}n + 2\lambda_{11}n}}{1 - \frac{\lambda_{12}n}{i\omega_n - \omega_0 - \lambda_{12}n + 2\lambda_{11}n}} \\ &= \frac{n}{i\omega_n - (\omega_0 + 2(\lambda_{12} - \lambda_{11})n)}.\end{aligned}\tag{3.17}$$

The lineshape at  $k = 0$  is a  $\delta$ -function just like for the non-interacting system, however, now the  $\delta$ -function is shifted to the frequency

$$\omega = \omega_0 + 2(\lambda_{12} - \lambda_{11})n.\tag{3.18}$$

Before proceeding further with the calculation of the lineshape for non-zero  $k$ , we would like to comment on why this particular set of diagrams, the ladder series, was chosen from all other possible sets. There are two justifications. First one is that any diagram that has two interaction lines crossing gives a much smaller contribution.



Such crossing diagrams represent processes in which more than two quasiparticles take part. These processes are at least of the same order as processes including ordinary elastic scattering, which we have neglected in this calculation so far.

The second justification is more subtle, yet important. The exact vertex part and the exact self-energy are not independent, and for an approximation scheme, it is desirable to have them consistent with each other [37]. This would make sure that all the results found for physical quantities in perturbation theory are obtained from the same free energy functional.

The approximation used here is known as the Random Phase Approximation [38, 46], and its self-consistent nature will be more transparent when we derive the transport equation in the next chapter.

We now turn to the evaluation of  $\Pi(k, \omega)$  when  $k$  is non-zero. As  $\Pi(k, \omega)$  for any  $k$  is algebraically related to  $\Pi'_0(k, \omega)$ , we just need to evaluate  $\Pi'_0(k, \omega)$  for arbitrary  $k$ . According to (3.7), one has

$$\Pi'_0(k, \omega_n) = - \int \frac{d^3p}{(2\pi\hbar)^3} \frac{n_B(p^2/(2m))}{\Delta\omega - \vec{p} \cdot \vec{k}/m}, \quad (3.19)$$

where

$$\Delta\omega = i\omega_n - \omega_0 + 2\lambda_{11}n - \lambda_{12}n - k^2/2m, \quad (3.20)$$

and  $n_B$  is the Bose distribution.

To evaluate the integral in Eq.(3.19) we separate the integration over  $d^3p$  into a one-dimensional integral over the component of  $p$  parallel to  $k$ ,  $p_{\parallel}$ , and a two-dimensional integral over the perpendicular components,  $p_{\perp}$ :

$$\Pi'_0(k, \omega_n) = - \int \frac{(dp_{\perp})(dp_{\parallel})p_{\perp}}{(2\pi)^2\hbar^3} \frac{1}{e^{p_{\perp}^2/(2mT)+p_{\parallel}^2/(2mT)} - 1} \frac{1}{\Delta\omega - p_{\parallel}k/m}. \quad (3.21)$$

The integral over the perpendicular components can be evaluated exactly, which gives

$$\frac{m^2T}{(2\pi)^2k} \int_{-\infty}^{\infty} dp' \frac{\ln(1 - e^{-p'^2})}{A - p'}, \quad (3.22)$$

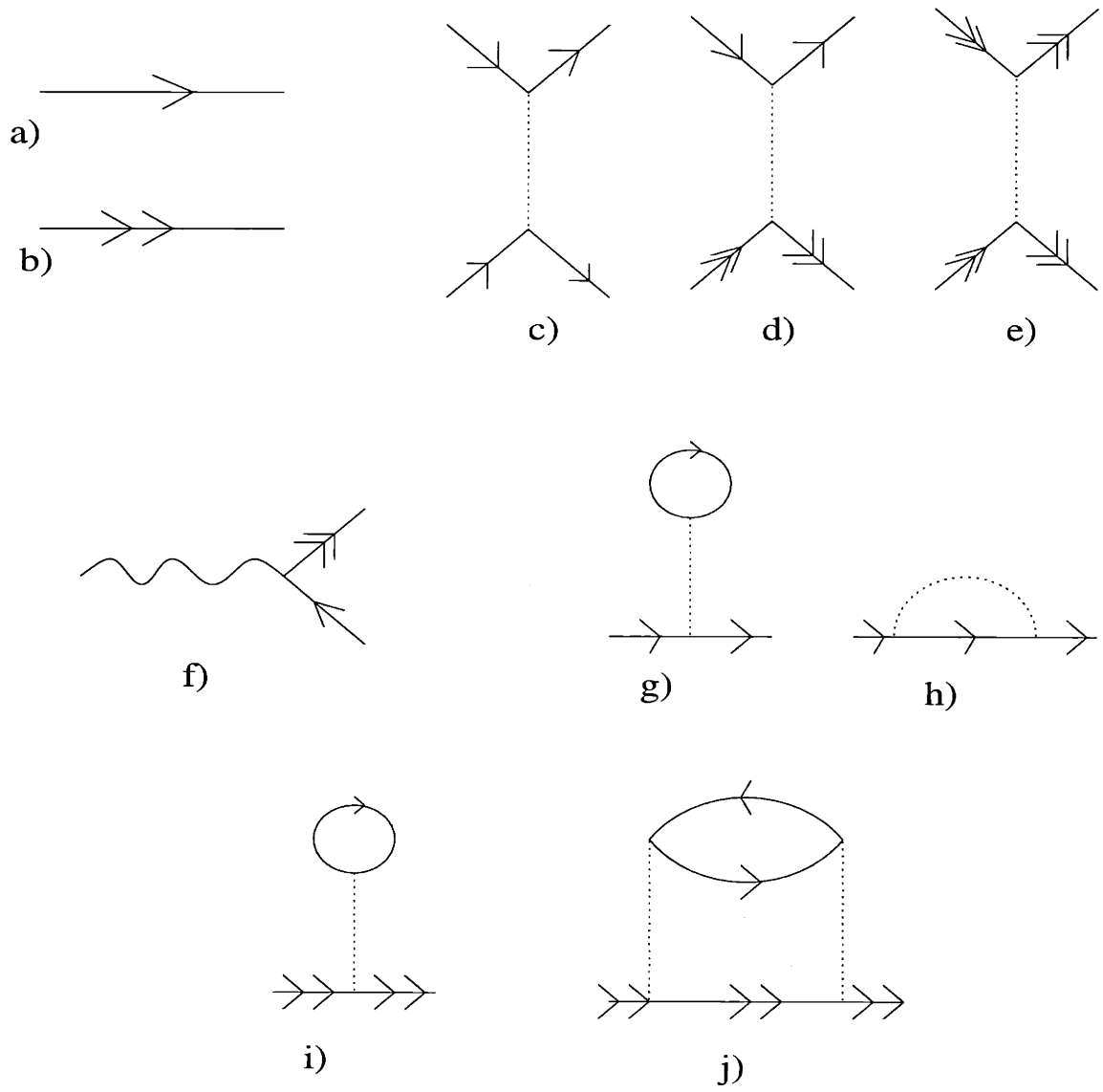


Figure 3-1: Various diagrams used in the calculation of the normal gas response.

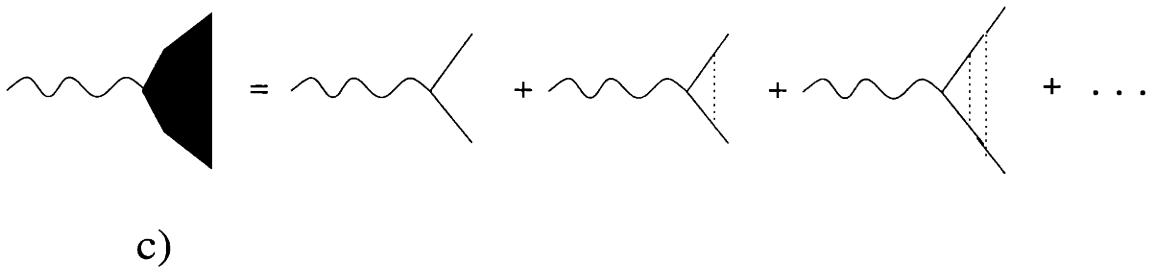
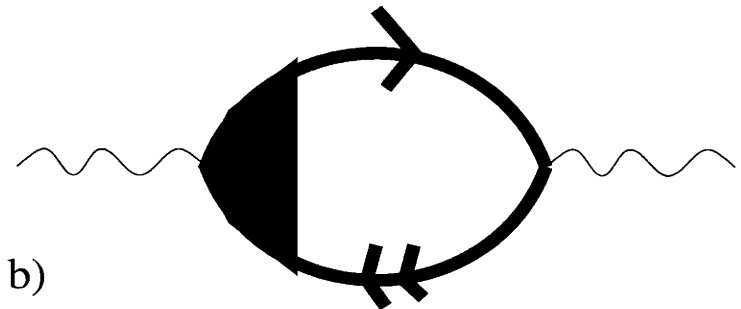
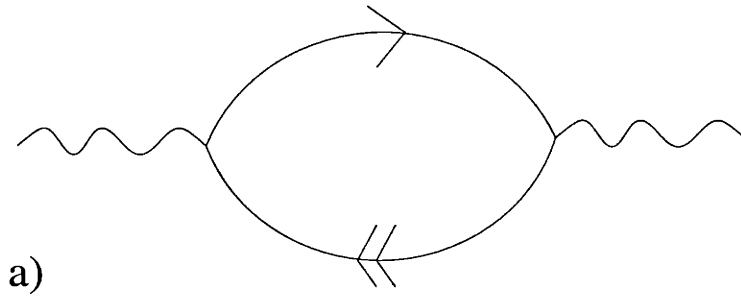


Figure 3-2: Diagrammatic representation of the ladder series approximation.

with

$$A = \frac{m\Delta\omega}{\sqrt{2mT}k}, \quad p' = p_{\parallel}/\sqrt{2mT}. \quad (3.23)$$

The integral in (3.22) cannot be evaluated exactly. Thus in order to calculate the lineshape, we convert the integral into a quickly converging series, and then numerically sum the series using the following procedure.

For an integral of the form

$$I(A) = - \int dx \frac{\ln(1 - e^{-x^2})}{x - A} \quad (3.24)$$

which is a convolution of  $\ln(1 - e^{-x^2})$  and  $x^{-1}$ , we employ Fourier transformation to write it in the form

$$- \int \frac{dp}{2\pi} f_1(p) f_2^*(p), \quad (3.25)$$

where

$$f_2(p) = \int dx \frac{e^{-ipx}}{x - A} = e^{-iAp} \theta(p). \quad (3.26)$$

For  $f_1$ , we have

$$f_1(p) = \int dx e^{-ipx} \ln(1 - e^{-x^2}). \quad (3.27)$$

After integrating by parts one has

$$f_1(p) = \frac{2}{ip} \int dx x e^{-ipx} \frac{e^{-x^2}}{1 - e^{-x^2}}. \quad (3.28)$$

To facilitate an expansion, we introduce two parameters  $a$  and  $b$  and replace the fraction in Eq.(3.28) by

$$\frac{1 - e^{-x^2}b}{1 + e^{-x^2}b} - \frac{1 - e^{-x^2}a}{1 + e^{-x^2}a}, \quad (3.29)$$

which gives us the desired result in the limit,  $a \rightarrow 1$ ,  $b \rightarrow 0$ . We then have

$$f_1(p) = \frac{2a}{ip(a-b)} \int dx \left( \tanh(x^2/2 - c_1/2) - \tanh(x^2/2 - c_2/2) \right) e^{-ipx} x, \quad (3.30)$$

with

$$c_1 = \ln(a) < 0, \quad c_2 = \ln(b) < 0. \quad (3.31)$$

Expanding the result in the poles of hyperbolic tangents and integrating we get

$$I(A) = \frac{a}{(a-b)} \sum_{n=-\infty}^{\infty} \ln \left[ \frac{\sqrt{|c_2| + 2\pi i n} - iA}{\sqrt{|c_1| + 2\pi i n} - iA} \right]. \quad (3.32)$$

The expansion is such that the discrete nature of the sum matters only for the small values of  $n$  (comparable to  $|c_2|/2\pi$ ), thus we carry out the sum over the first  $n^*$  terms, and convert the rest of the sum to an integral which can be evaluated exactly. This approximation works very well even if  $n^*$  is a reasonably small number, which we have verified by comparing numerical results for various values of  $n^*$ .

The resulting lineshape (3.15) is displayed in figure Fig.(3-3) for different values of  $k$  and density  $n$ . In the next section we will analyze the features of the lineshape, and discuss some of the underlying physics of the presented calculation.

## 3.2 Predictions for the Spectrum

### 3.2.1 The dispersion relation

From the result plotted in Fig.(3-3). we see that the lineshape consists of a peak, embedded in a broad, incoherent background. Here, we will be interested in two features of this lineshape, the position of the peak, and the mean frequency or the average density shift, defined as the center of mass of the spectrum, including both the peak and the background.

We start by investigating the latter feature. We define the average density shift as

$$\bar{\omega}_k = \frac{\int d\omega \omega \mathcal{I}(k, \omega)}{\int d\omega \mathcal{I}(k, \omega)}. \quad (3.33)$$

We have seen that for  $k = 0$ , the lineshape is a  $\delta$ -function at  $\omega = \omega_0 + 2(\lambda_{12} - \lambda_{11})n$ .

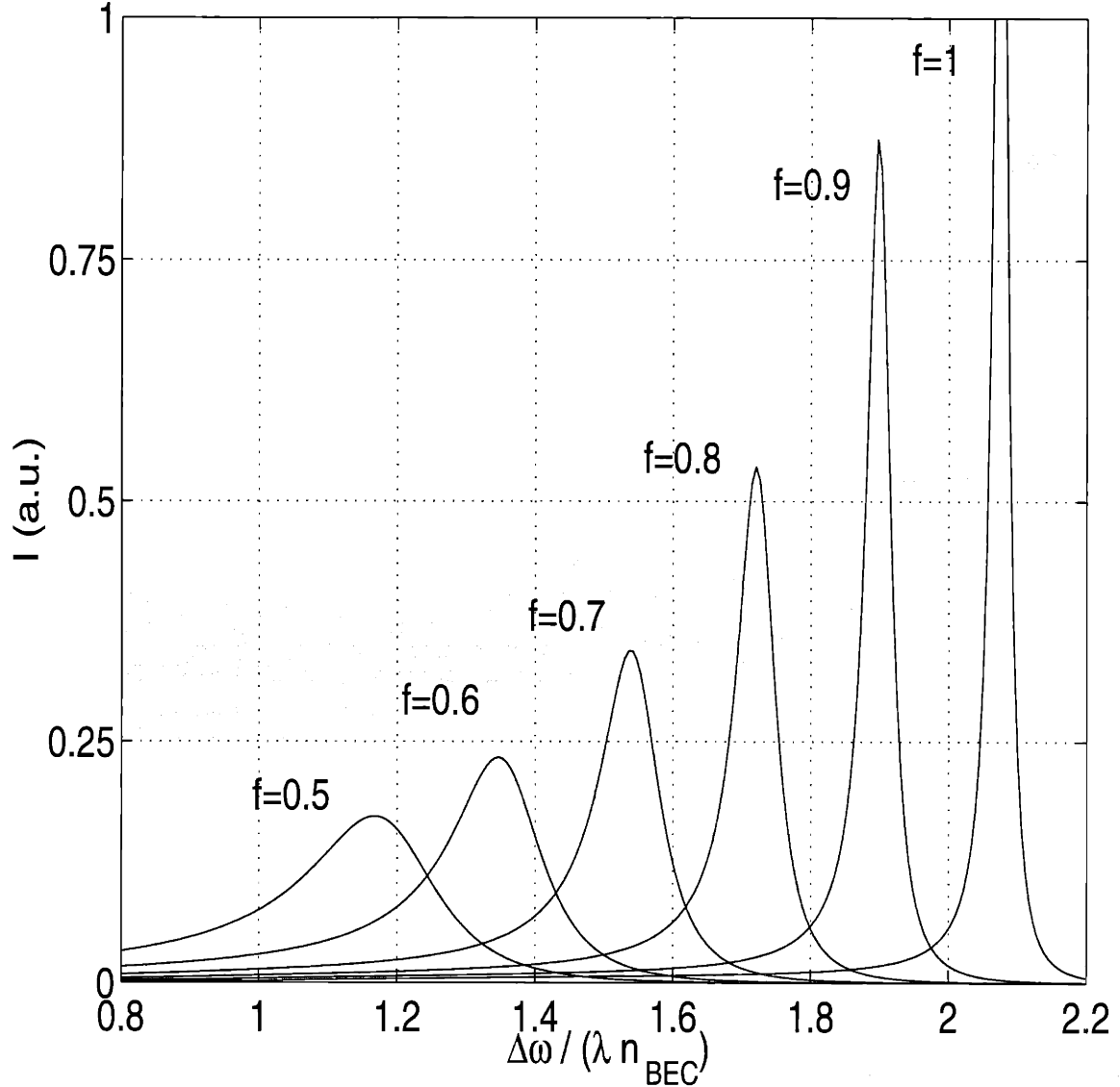


Figure 3-3: Absorption spectrum above BEC at fixed temperature and varying density:  $n = fn_{\text{BEC}}$ ,  $0.5 \leq f < 1$ . The frequency shift  $\Delta\omega$  is defined relative to the that of a free atom at rest:  $\Delta\omega = \omega - \omega_0 - k^2/2m$ . Spectral power  $\mathcal{I}$  is normalized by particle density  $n$ . The excitation wavevector  $k$  is 0.5 in the units of  $\lambda_{12}n_{\text{BEC}}/v_T$ . The interaction constant  $\lambda_{11}$  is chosen to be 0. Note that the peak position follows the relation (3.40).

Thus, the mean frequency is

$$\bar{\omega}_{k=0} = \omega_0 + 2(\lambda_{12} - \lambda_{11})n. \quad (3.34)$$

To extend this calculation to finite values of  $k$ , we recall the expansion

$$\Pi(k, \omega) = \Pi'_0 + \lambda_{12}(\Pi'_0)^2 + \dots \quad (3.35)$$

Upon making analytic continuation to get the retarded Green's functions [36], we obtain

$$\int d\omega \text{Im}\{\Pi^R(k, \omega)\} = \text{Im}\left\{\int d\omega \left[\Pi_0'^R + \lambda_{12}(\Pi_0'^R)^2 + \dots\right]\right\}. \quad (3.36)$$

To evaluate the integral, we can close the contour over the upper half plane. We know that, being causal functions, all  $\Pi^R(\omega)$  have all their poles in the lower half plane, and at large  $\omega$  behave as  $1/\omega$ . Thus, all the terms except the first one give zero. And we obtain,

$$\int d\omega \mathcal{I}(k, \omega) = -\pi n. \quad (3.37)$$

Similarly the numerator of (3.34) can be evaluated with the same method of expanding in powers of  $\Pi'_0(\omega)$ . Putting these results into Eq.(3.34) we have

$$\bar{\omega}_k = \omega_0 + 2(\lambda_{12} - \lambda_{11})n + \frac{\hbar^2 k^2}{2m}. \quad (3.38)$$

Note that the average density shift is independent of temperature, and varies linearly with the density. Furthermore, the effect of finite momentum transfer to the particle effects the average shift only through the free particle kinetic energy.

Even though such simplicity may seem to arise from the simplicity of the model used to describe the system, it turns out that the average density shift is related to some basic properties of the system. We will relax the assumption of homogeneity and even thermal equilibrium, and give a general sum rule for the average shift of an optical spectrum in chapter 6.

Our next goal in this section in this section is to study the peak in

the absorption spectrum given by the pole of  $\Pi(k, \omega)$ . As one can see from the result at  $k = 0$ , for spatially uniform excitation the peak position is given by Eq.(3.34) with  $k = 0$ . However as we now show, at finite  $k$  there is no direct relation between the average frequency shift  $\bar{\omega}_k$  and the peak position. This is not surprising because at finite  $k$  the spectrum contains a smooth background as seen in Fig.(3-3).

The peak is well defined only when the density shift  $\lambda_{12}n$ , is much larger than the Doppler broadening  $v_T k$ . Then in this limit we expand  $\Pi'_0(k, \omega)$  in powers of  $\frac{v_T k}{\lambda_{12}n}$ ,

$$\begin{aligned} \Pi'_0(k, \omega) &= - \int d^3p \frac{n_B(p^2/2m)}{\Delta\omega - \vec{k} \cdot \vec{p}/m} \\ &\simeq - \int d^3p \frac{n_B(p^2/2m)}{\Delta\omega} + \frac{1}{(\Delta\omega)^2} \int d^3p n_B(p^2/2m) (\vec{k} \cdot \vec{p}/m)^2 \\ &\simeq -n/(\Delta\omega) + \frac{1}{3} \left( \frac{v_T k}{\lambda_{12}n} \right)^2. \end{aligned} \quad (3.39)$$

The factor 1/3 arises from the angular integration.

Putting this result back to the expression (3.15) for  $\Pi$ , we get the pole of the response function at

$$\omega = \omega_0 + 2(\lambda_{12} - \lambda_{11})n + \hbar^2 k^2 / 2m + \frac{1}{3} \frac{v_T^2}{\lambda_{12}n} k^2. \quad (3.40)$$

Note that since  $\frac{v_T^2}{\lambda_{12}n} \gg 1/m$ , the dispersion that is caused by the exchange interaction  $\lambda_{12}$  is much stronger than the dispersion caused by the free movement of the particles. This dispersion is a collective effect, which gives the optical mode an effective mass much lighter than the free particle mass.

For all values of  $k$ , such that the peak is narrow enough to permit the definition of a peak position, this peak is at  $\omega$  given by Eq.(3.40). Thus this expression is justified by the calculated lineshape.

### 3.2.2 Broadening

Broadening of the optical spectrum is due to two major mechanisms: Elastic scattering and Landau damping. The relative importance of these effects depends on the



relation between the density  $n$ , temperature  $T$ , and interaction  $\lambda$ .

Whenever two particles in the gas go through a collision in which both of them change their momenta to new values (all the collision events except forward and backward scatterings), any correlation between the internal states and the momentum states is lost. It was argued in the introduction that the rare occurrence of these events at low temperatures, with a mean frequency of

$$\tau_{el}^{-1} = 8\pi a^2 v_T n, \quad (3.41)$$

made the coherence of the wavefunctions important in the calculation of the optical spectrum.

This effect can be properly taken into account by adding a new class of diagrams to both the self-energy parts  $\Sigma(k, \omega)$  and the vertex part  $\Gamma(k, \omega)$ . However, as these effects are small, we estimate this broadening by adding a the self-energy part shown in Fig.(3-1 j). As a result, even when the external field is uniform, the spectrum, instead of a  $\delta$ -function will be a Lorentzian, with a width,

$$\gamma \simeq \tau_{el}^{-1}. \quad (3.42)$$

Another broadening effect appears even when one neglects elastic collisions. This mechanism is the transfer of energy from the collective mode to single particles and is called Landau damping [38]. This effect was considered in the calculation shown in this chapter, and is the reason why the lineshapes shown in the figure Fig.(3-3) are not infinitely sharp.

We can calculate the width of the optical resonance due to Landau damping as follows. Recalling

$$\Pi(k, \omega) = \frac{\Pi'_0}{1 - \lambda_{12}\Pi'_0}, \quad (3.43)$$

we can write

$$\text{Im}\Pi(k, \omega) = \frac{\text{Im}\Pi'_0}{(1 - \lambda_{12}\text{Re}\Pi'_0)^2 + \lambda_{12}^2(\text{Im}\Pi'_0)^2}. \quad (3.44)$$

We know that for small  $k$ , the peak will be centered near  $\omega_k$  given by Eq.(3.40). Thus

we can approximate,

$$\text{Re}\Pi'_0(\omega) \simeq \frac{n}{\Delta\omega}, \quad \Delta\omega = \omega - \omega_0 + 2\lambda_{11}n - \lambda_{12}n. \quad (3.45)$$

The imaginary part of  $\Pi'_0(\omega)$  can be calculated by expanding in the same parameter  $\frac{v_T k}{\lambda_{12}n}$  as,

$$\text{Im}\Pi'_0 \simeq \frac{\sqrt{\pi}n}{v_T k} e^{-\left(\frac{\lambda_{12}n}{v_T k}\right)^2}. \quad (3.46)$$

Substituting these expressions into the formula for the imaginary part of  $\Pi$ , we get an approximate lineshape which is correct in the vicinity of  $\omega_k$ . Calculating the full width at half maximum of this lineshape gives us a broadening of

$$\gamma = \sqrt{\pi} \left(\frac{\lambda_{12}n}{v_T k}\right)^2 v_T k e^{-\left(\frac{\lambda_{12}n}{v_T k}\right)^2}. \quad (3.47)$$

The characteristic feature of this result is that there is an exponential narrowing of the line width relative to the usual Doppler broadening of  $v_T k$ . The narrowing of the line with decreasing temperature is not surprising, however, narrowing of the line caused by increasing density deserves more explanation.

It was first pointed out by Dicke [13], that when collisions in a system do not disturb the optical coherence, increasing the density of the system results in the narrowing of the lines. A similar mechanism is responsible for the narrowing in our case. However, the functional form of the linewidth on wavevector is different. We can explain the difference in technical terms by noting that in our theory of the optical spectrum, we consider ladder diagrams in which each block is independent. Physically this means that the velocity of the excited particle is randomized every time it interacts with the surrounding particles through an exchange process. Such randomization of the velocity results in a shorter travel distance throughout the excitation, and thus a narrowing of the line. We will discuss the physics of the narrowing phenomenon with more care in the next chapter. In the rest of this chapter we concentrate on the case of Bose condensation.

### 3.3 Optical Spectrum Below Bose-Einstein Condensation

When the temperature is low enough, a system of bosons goes through a phase transition. The physical reason for this transition is large overlap of the de Broglie wavefunctions of the particles, and their tendency to be in the same state. For a homogeneous, non-interacting Bose gas, a finite fraction of the particles occupies the ground state, when the temperature is reduced below a critical value,

$$T_c = \zeta(3/2)\hbar^2 n^{2/3}/m. \quad (3.48)$$

These particles form the Bose-Einstein condensate, and the appearance of a condensate qualitatively modifies many physical properties. It is our aim in this section to understand how the optical spectrum of a dilute system is modified by Bose Einstein condensation [29].

Before entering the discussion we recall that an important change takes place in the low energy part of the quasi-particle dispersion relation. The dispersion relation which is quadratic above Bose condensation, becomes linear at low energies [34]. Switching from linear to quadratic behavior takes place at a length scale determined by the condensate density and interactions,

$$\zeta = \sqrt{\hbar^2/(2m\lambda_{11}n)}. \quad (3.49)$$

If one is not interested in very low temperatures, of the order of

$$T^* \simeq \hbar^2/(\zeta^2 2m) = \lambda_{11}n, \quad (3.50)$$

the deviation from the quadratic behavior in the quasiparticle spectrum can be safely neglected. Therefore we assume that the free Green's function for particles in state 1 or state 2 are not changed. Thus our theory will be valid for all temperatures between  $T^*$  and  $T_c$ .

Our task will be to add the presence of the condensate to the perturbation theory developed in the previous sections. We accomplish this by using the diagrammatic approach once again, this time including the number operators of the condensate in our diagrams by the Beliaev method [2, 8].

The calculation will go along the lines of the calculation done for  $T > T_c$ . However, with the new diagrammatic possibility of introducing two condensate lines to replace a Green's function for state 1, one has to sum a larger set of diagrams.

First, there is a new self-energy part involving forward scattering process from the condensate density, which gives a contribution of  $\lambda_{11}n_c$  ( $\lambda_{12}n_c$ ) to the denominator of the state 1 (state 2) Green's function (see Fig.(3-4 b,c). This however is not the only place where the condensate operators come into calculation.

Similar to the non-condensed case, we first start by considering a non-interacting system. Then, only two diagrams contribute to the response function,

$$\Pi = \Pi_0 + \Pi_c. \quad (3.51)$$

The expression for  $\Pi_0$  is not different from what was obtained in the previous calculation. The condensate contribution  $\Pi_c$  (see Fig.(3-4 a), is given by

$$\Pi_c(k, \omega) = n_c \mathcal{G}_{II}(k, \omega). \quad (3.52)$$

When the interaction is turned on, one has to sum a ladder series similar to Eq.(3.14). Here the difference is that each link of the ladder can be either  $\Pi_0$  or  $\Pi_c$  (see Fig.(3-4 e) as one example). Furthermore two diagrams where two  $\Pi_c$  are adjacent should be excluded from the sum. These diagrams have already been counted by the introduction of the self-energy part due to direct processes with the condensate.

We perform this summation by summing two geometric series in succession. Let us define

$$\Pi_e = \Pi_0 + \lambda_{12}(\Pi_0)^2 + \dots = \frac{\Pi_0}{1 - \lambda_{12}\Pi_0}. \quad (3.53)$$

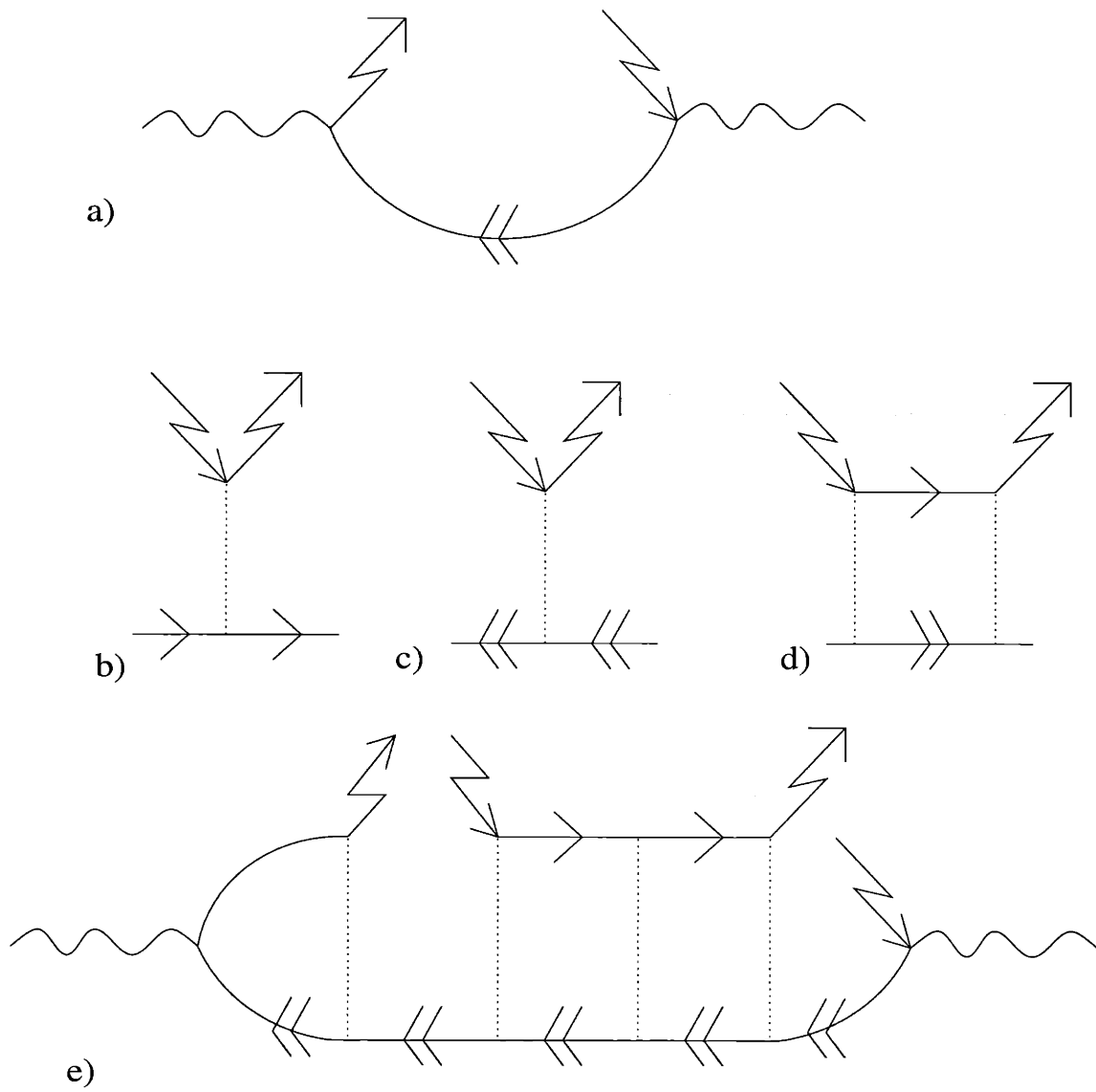


Figure 3-4: Various diagrams used in the calculation of the condensate response.

Then the total response function can be resummed in terms of  $\Pi_e$  as follows:

$$\begin{aligned}
\Pi &= \Pi_e + (1 + \Pi_e)\Pi_c(1 + \Pi_e) + (1 + \Pi_e)\Pi_c\Pi_e\Pi_c(1 + \Pi_e) \\
&+ (1 + \Pi_e)\Pi_c\Pi_e\Pi_c\Pi_e\Pi_c(1 + \Pi_e) + \dots \\
&= \Pi_e + \frac{(1 + \Pi_e)\Pi_c(1 + \Pi_e)}{1 - \Pi_c\Pi_e},
\end{aligned} \tag{3.54}$$

which is the desired result for the optical response.

As in the non condensed case, we first look at the response for a uniform excitation,  $k = 0$ . We see that the spectrum in this case consists of two  $\delta$ -functions. The frequencies of the location of the  $\delta$ -functions are given by

$$\omega_{1,2} = \omega_0 + (\lambda_{12} - 2\lambda_{11})n + \Delta\omega_{1,2}. \tag{3.55}$$

Here  $\Delta\omega_{1,2}$  are the roots of the quadratic equation,

$$(\Delta\omega_{1,2} - \lambda_{11}n_c)(\Delta\omega_{1,2} - \lambda_{12}n_T) = \lambda_{12}^2 n_c n_T. \tag{3.56}$$

The strengths of the two peaks depend on the temperature and generally are not equal. The fraction of the spectral weight in the stronger peak can be expressed in terms of the condensate fraction  $f = n_c/n$  as

$$\begin{aligned}
\mathcal{I}_1 &= \frac{\int_{\omega_2-\epsilon}^{\omega_2+\epsilon} d\omega \mathcal{I}(\omega)}{\int d\omega \mathcal{I}(\omega)} \\
&= \frac{(1-f)(1/2+f) + \frac{1}{2}\sqrt{(1+f)(1-3f)}}{\sqrt{(1+f)(1-3f)}}.
\end{aligned} \tag{3.57}$$

Let us qualitatively describe the evolution of  $k = 0$  spectrum, as the temperature is lowered from  $T_c$ . At  $T_c$ , we have only one peak at the frequency

$$\omega_2 = \omega_0 + 2(\lambda_{12} - \lambda_{11})n. \tag{3.58}$$

Thus the optical spectrum evolves continuously through the transition. This means

that the peak at  $\omega = \omega_2$  is associated with the atoms above the condensate, and henceforth we will refer to it as the normal peak. The second peak appears as soon as the temperature is lowered below  $T_c$ , at the frequency

$$\omega_1 = \omega_0 + (\lambda_{12} - 2\lambda_{11})n. \quad (3.59)$$

However, this peak is much weaker than the normal peak. Close to the transition, this strength is linear in the condensate density, which shows that this resonance measures the response of the atoms in the condensate. We will refer to the peak at  $\omega = \omega_1$  as the condensate peak. The absence of the exchange contribution for the condensate peak is discernible in the  $\lambda_{12}n$  difference between the frequencies of the two peaks.

As the temperature is lowered further below  $T_c$ , the strength of the condensate peak grows, however, it always remains weaker than the normal peak. The frequencies of the two peaks first repel each other, which is a clear indication that the condensate response is coupled to the normal response. This mixing eventually causes the peaks to converge, and at  $T = 0$ , both peaks are at the frequency

$$\omega_1 = \omega_0 + (\lambda_{12} - 2\lambda_{11})n, \quad (3.60)$$

and have equal strength. This is not surprising, since at zero temperature there are no atoms left in the normal part, and all the response is due to the condensate.

Another quantity of interest is the average frequency shift, defined in Eq.(3.34). We find that it is given by

$$\bar{\omega}_{k=0} = \omega_0 + (\lambda_{12} - 2\lambda_{11})n + \lambda_{12}n(1 - f^2). \quad (3.61)$$

By using arguments similar to those given for the normal gas one can generalize this result to non-zero  $k$ :

$$\bar{\omega}_k = \omega_0 + (\lambda_{12} - 2\lambda_{11})n + \lambda_{12}n(1 - f^2) + \frac{\hbar^2 k^2}{2m}. \quad (3.62)$$

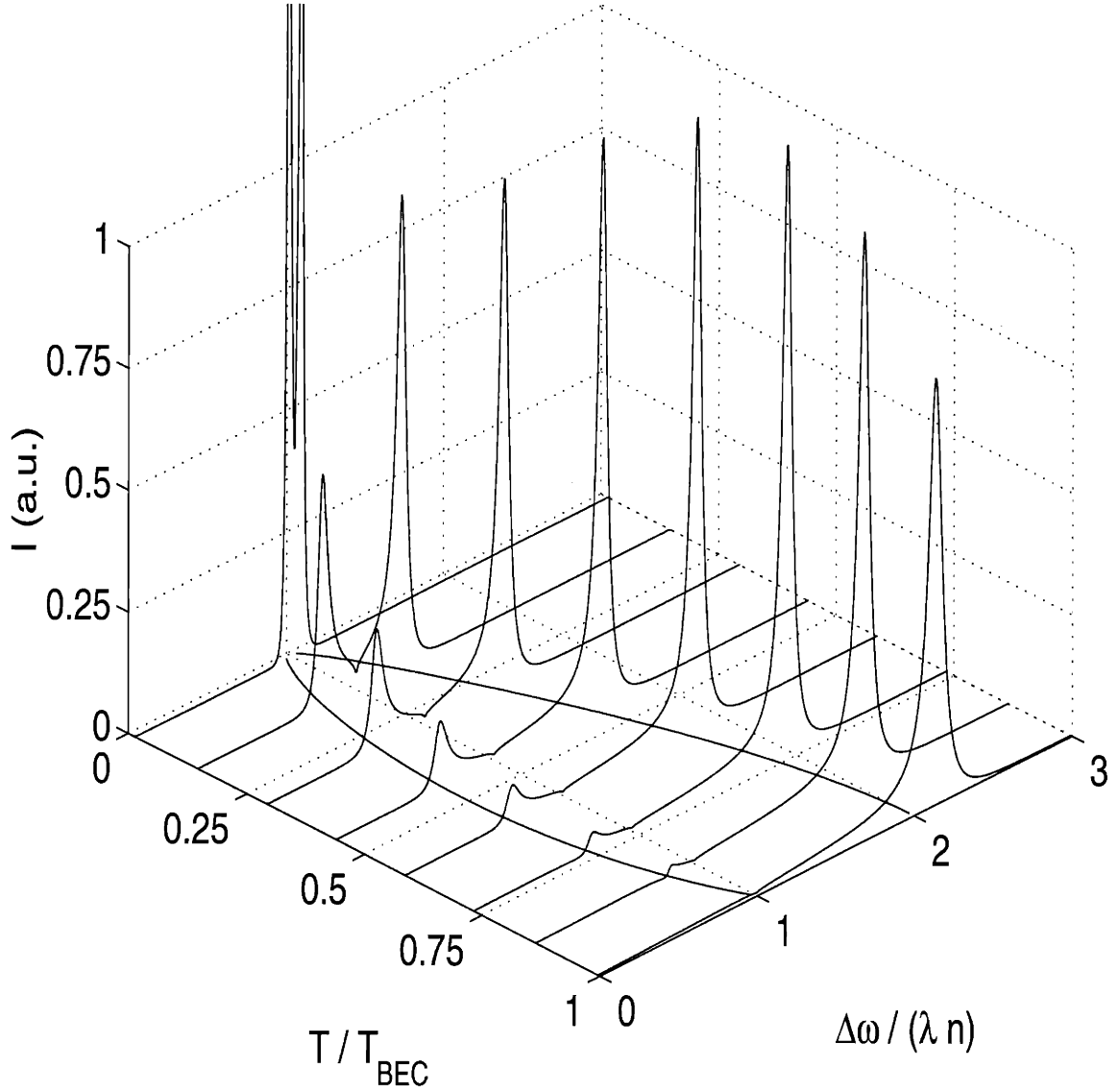


Figure 3-5: Absorption spectrum in the BEC regime, shown for temperature varying between 0 and  $T_c$ ; density  $n$  fixed. The excitation wavevector  $k$  is  $2/3$  in the units of  $\lambda_{12}n/v_T$ . Lines in the base plane indicate the peak positions for  $k = 0$  (3.56). Note narrowing of the spectral line with decreasing  $T$ , and strengthening of the condensate peak due to increasing condensate fraction. (The frequency shift  $\Delta\omega$  is defined in Fig.3-3;  $\lambda_{11} = 0$ .)



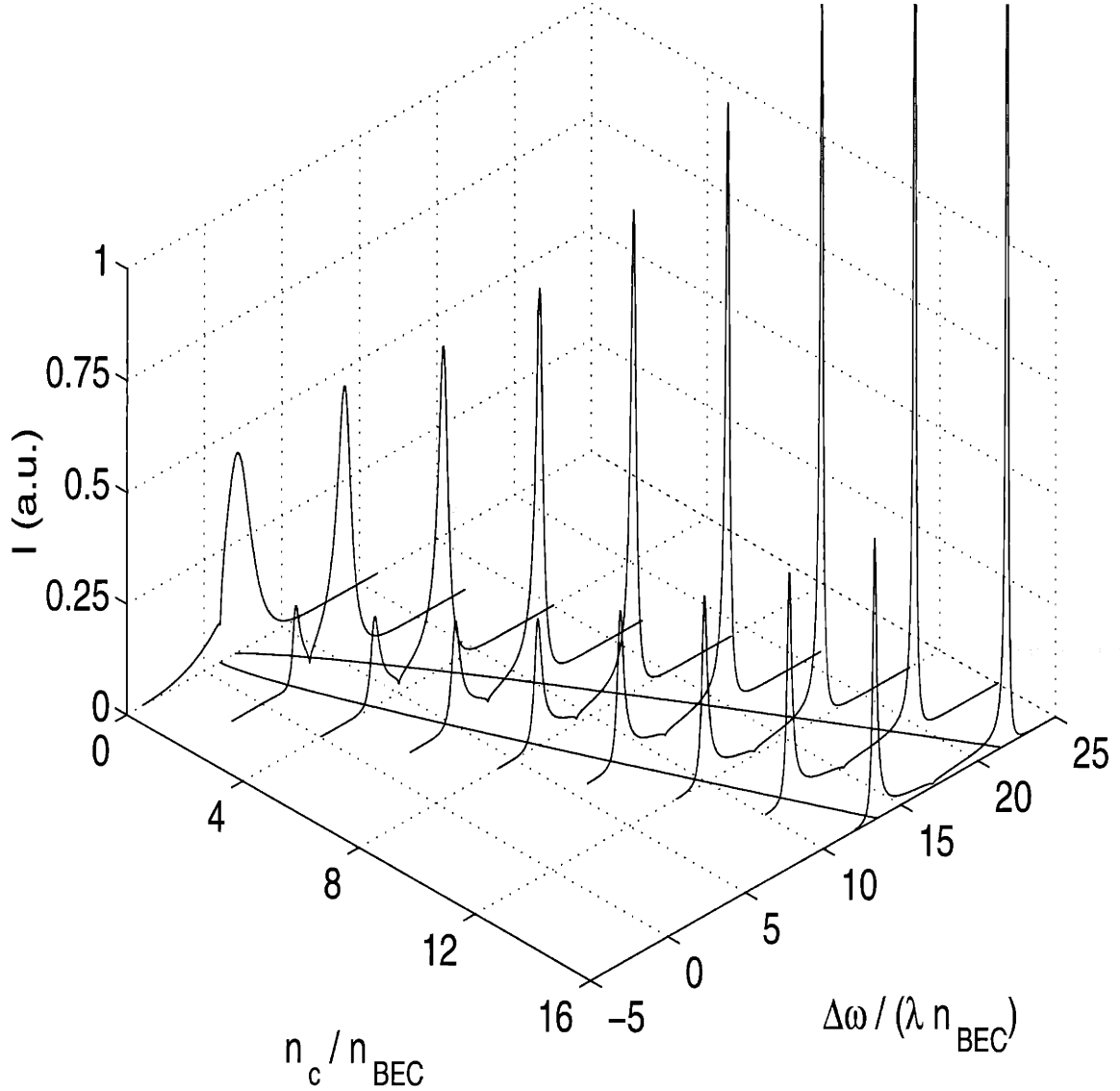


Figure 3-6: Absorption spectrum in the BEC regime at fixed temperature and density varying from  $n_{\text{BEC}}$  and up. Excitation wavevector  $k = 2.5$  in the units of  $\lambda_{12} n_{\text{BEC}} / v_T$ . Increasing condensate density leads to narrowing of the peaks and to strengthening of the condensate peak, as in Fig.3-3. ( $\Delta\omega$  and  $\mathcal{I}$  are defined in Fig.3-3;  $\lambda_{11} = 0$ .)

These result (3.62) is special cases of a more general sum rule given in Chapter 5.

The calculation of the full response function  $\Pi(k, \omega)$  for finite  $k$  is carried out using the same procedure as that described for the normal gas. The results are given in figures Fig.(3-5,3-6) . The two important features we found for the normal gas spectrum can also be observed here. First, the dispersion of the peaks with  $k$ , is present again for the condensed case. However, this dispersion is due to the atoms above the condensate, and it is more prominent for the normal peak than the condensate peak. Also, the narrowing of both peaks takes place as the gas density is increased, as Fig.(3-6) clearly shows.

Another important effect is the change in the elastic lifetime below condensation. In the normal gas, the elastic lifetime is solely due to collisions with the normal gas atoms, while here there is another possibility. The excitation of atoms from the condensate to the normal gas also gives a contribution, which becomes more significant as the temperature is lowered. This effect is represented by the self-energy part  $\Sigma_c$  shown in Fig.(3-4).

We find that this contribution to self-energy is imaginary and scales with  $(a/\lambda_T)^{4/3}$ , which is still somewhat weaker than the  $(a/\lambda_T)$  frequency shift effects we are concerned with here. However, it is more pronounced than the  $(a/\lambda_T)^2$  ordinary elastic lifetime. Near  $T = 0$  we can estimate the broadening as,

$$\gamma_{el} \simeq 8\pi v_T a^2 n_T + \left(\frac{a}{\lambda_T}\right)^{4/3} T_c. \quad (3.63)$$

This completes our discussion of diagrammatic calculation of the optical response. In the next chapter, we use the transport equation to discuss some of the effects found in this chapter, and give alternative derivations for them.

# Chapter 4

## Collective Properties of Optical Excitations

We have seen in Chapter 3 that the optical spectrum obtained for a cold gas is qualitatively different from that of a classical dilute gas. In particular, we have found that the lineshape is strongly affected by interparticle interactions. Also, the dispersion relation for the optical modes arising due to interactions is a result that can not be reconciled within the usual one particle description of an optical excitation as a transition between two internal states of a single particle. Instead, one has to think of excitation as of a process in which many particles participate. It will be our aim in this chapter to clarify the nature of this participation and the origin of these collective effects.

We shall start with a discussion of the difference between a cold gas ( $\lambda_T > a$ ) and a classical gas. Consider what happens when a particle is taken out of a momentum state  $k$  of a gas in thermal equilibrium, thus creating a “hole” in the equilibrium distribution. We are interested in how long it will take for this hole to be filled. In both the classical gas and the quantum gas, the hole will be filled by a particle that undergoes a collision and ends up in the  $k$  state. Thus one needs to look more closely at collision processes.

Two particles in momentum states  $k_1$  and  $k_2$ , after collision will end up in the states  $k_3$  and  $k_4$ , satisfying  $k_1 + k_2 = k_3 + k_4$ . We can have  $(k_1, k_2) \neq (k_3, k_4)$ , when

both particles scatter into momentum states different from the initial ones. We call such collisions ordinary elastic collisions, and note that it is through these collisions that the momentum distribution of the gas relaxes. There are, however, two other possibilities for the outcome of a collision. First is when the momentum states of the particles remain unchanged,  $k_1 = k_3$ ,  $k_2 = k_4$ . This is forward scattering, related to the forward part of the two particle scattering amplitude. The second possibility is that the particles exchange their momenta  $k_1 = k_4$ ,  $k_2 = k_3$ . This is backward scattering, its name corresponding to the picture in the center of mass frame.

In general, the rate of ordinary elastic collisions is different from the rates of forward and backward processes. And for bosons, the rates of forward and backward processes are equal. These rates are calculated in the chapter 3, when the interaction potential is substituted by a  $\delta$ -function in the pseudo-potential approximation [20]. We have, for forward and backward collisions

$$w_{coh} = \tau_{coh}^{-1} = \frac{4\pi\hbar a}{m} n = \lambda n, \quad (4.1)$$

and for ordinary elastic collisions,

$$w_{el} = \tau_{el}^{-1} = 8\pi a^2 v_T n. \quad (4.2)$$

The relative importance of these processes can be estimated by comparing (4.1) and (4.2),

$$\frac{w_{el}}{w_{coh}} \simeq \frac{a}{\lambda_T}. \quad (4.3)$$

Thus, the ratio of scattering length to the thermal de Broglie wavelength measures the significance of ordinary collisions compared to coherent collisions.

The condition which holds for the quantum gas  $\lambda_T \gg a$ , ensures that any particle in the quantum gas will experience many backward and forward scatterings before it is scattered into another momentum state by an ordinary elastic collision. Therefore interparticle interactions effect the optical spectrum mainly through the forward and backward processes in a quantum gas, but only through ordinary elastic collisions in

a classical gas. This is the physical reason why the results for a quantum gas are so different from the classical case.

The expression (4.1) for forward and backward processes rates has two important properties. Firstly, it is linear in the scattering length  $a_s$ , and secondly it is independent of temperature. Understanding these properties would clarify the nature of these processes.

A simple physical picture for a forward collision enables us to understand both of these properties. We have seen that the momentum state of the particle does not change in a forward collision, thus, the trajectory of a particle going through only forward collisions is not different from a particle in an ideal gas. However, the particle moving along this trajectory is still subject to the potential of all the other particles in the gas. This potential, averaged over the trajectory, would make the phase of the wavefunction of the particle increase at a different rate than in an ideal gas. A phase difference of  $w_{coh}t$  would accumulate between the two cases after a time  $t$ . Thus, forward collisions effect only the phase of the wavefunction, and this phase difference is linearly proportional to how strong the potential of the other particles is. The strength of the potential is linearly (not quadratically) proportional to the scattering length, which explains why  $w_{coh}$  depends linearly on the scattering length  $a$  and the density,  $n$ . Also, in this picture the speed of the particles in the gas is not important, so it is expected that the resulting phase is independent of temperature.

For such a picture to hold, we must assume that the trajectory of the particle traversed in a single momentum state is long enough for the appropriate averaging to take place. This is equivalent to requiring  $w_{coh}t \gg 1$ . Here,  $t$  should be taken as  $\tau_{el}$ , the elastic mean free time. We then see that the quantum gas condition is also the condition for the length of the trajectory, validating our picture.

The interpretation of the backward rate  $w_{coh}$  is more subtle. For bosons, the quantum mechanical amplitude of backward s-wave scattering is equal to the forward scattering amplitude. As going through a backward collision the particle changes its momentum state, the rate  $w_{coh}$  is the rate of coherent hopping of the excited particle in momentum space.

After realizing that it is the backward and forward scattering processes that are dominant in a quantum gas, we now discuss how they effect the optical spectrum.

Consider a quantum gas with all particles in internal state 1. We would like to understand evolution of a particle's momentum state while its internal state changes under the action of an external field. For simplicity, we assume that the external field is uniform, so that the optical absorption changes only the internal state, leaving the translational (momentum) state the same.

After the internal state change takes place, the excited particle will evolve coherently over a time on the order of  $\tau_{el}$ , experiencing many backward and forward scatterings. However, we have seen previously that at this time scale, we need to consider not just the excited particle, but also the hole it leaves behind in the momentum distribution of state 1 particles. We must then investigate how this state 2 particle-state 1 hole pair goes through forward and backward processes.

Evidentially, in a forward collision the momentum state of the particle in state 2 does not change, and neither does that of the state 1 hole. Thus the pair's coherence is not disturbed by forward collisions. What is more important is that, this coherence is not effected by backward scattering, either. When the state 2 particle in momentum state  $k_1$  exchanges its momentum with a state 1 particle at  $k_2$ , this particle fills the initial hole at  $k_1$ . However, now a hole is created at  $k_2$ , accompanying the state 2 particle.

Thus, the picture we have for the optical excitation in a quantum gas is a particle-hole pair, coherently changing momentum states. This picture shows that many momentum states must be considered in the calculation of the optical response. It is also crucial to account not only for the particle in the excited state, but also for the hole left in the ground state distribution, as well as for the correlation between them.

It is useful to point out that this correlation between the excited particle and the accompanying hole is a consequence of the dynamical equations, and not a result of some attraction between them causing the formation of a bound state. The hole stays in the same momentum state as the excited particle, since uniform excitation field does not transfer momentum to the system. Thus the excited particle "inherits"

the spatial wavefunction of the initial state 1 particle. One would then expect this correlation to diminish when the excitation is carried out using a non-uniform field. In Chapter 3 the quantity which signified this correlation was the fraction of the spectral weight present in the main peak of the optical response [39]. Indeed one can see in Fig(3-3) that upon increasing the excitation field wave vector  $|k|$ , a significant background appears in the spectrum, reducing the spectral weight in the peak.

Thus, whenever the excited particle is allowed to make many exchange scatterings, the optical mode becomes a collective mode. The excitation is shared by many particles, in different momentum states.

A similar argument has been given by Bashkin, Lhullier and Laloë and [6, 32, 33, 7], in the context of spin waves in dilute gases. Specifically in [43], Pinard and Laloe consider the scattering matrix for two particles in non-orthogonal spin states. They find that due to the coherent processes described above, the spins of the two atoms precess around each other during the collision. Our problem, by going to a two state internal space Bloch spin representation [11], is mapped on an equivalent spin problem.

## 4.1 Transport Equation

The concept of a collective mode is conventionally defined by specifying a quantity that harmonically oscillates in space and time [39]. For sound waves this quantity is particle density, for spin waves it is the density of a component of spin in some particular direction, etc. In this section, we will describe the quantity that forms the collective optical excitations - the off-diagonal part of the internal state density matrix.

To obtain a clear real space picture, we now derive the transport equation. We start by rewriting the Hamiltonian in terms of the real space field operators as

$$\mathcal{H} = \int d^3r \sum_{\alpha} \psi_{\alpha}^{+}(r) \left( -\frac{\hbar^2 \nabla^2}{2m} + \hbar U_{\alpha}(r) \right) \psi_{\alpha}(r) \quad (4.4)$$

$$+ \int d^3r \sum_{\alpha,\beta} \frac{\hbar\lambda_{\alpha\beta}}{2} \psi_{\alpha}^{\dagger}(r) \psi_{\beta}^{\dagger}(r) \psi_{\beta}(r) \psi_{\alpha}(r).$$

The indices  $\alpha, \beta$  run over the internal states 1,2. We have also allowed for an external potential  $U_{\alpha}(r)$ , which includes the energy of the internal state  $\hbar\omega_{\alpha}$ . Interaction parameters  $\lambda_{\alpha\beta}$  have been defined in Chapter 2. The operators  $\psi$  satisfy the bosonic commutation relations,

$$[\psi_{\alpha}(r), \psi_{\beta}^{\dagger}(r')] = \delta_{\alpha\beta} \delta(r - r'). \quad (4.5)$$

Transitions between the internal states will be caused by an excitation field, which gives another term of the Hamiltonian,

$$\mathcal{H}_{\text{exc}} = \sum_{\alpha\beta} \int d^3r A_{\alpha\beta}(r, t) \psi_{\alpha}^{\dagger}(r) \psi_{\beta}(r), \quad (4.6)$$

where we assume harmonic variation in space and time,

$$A_{\alpha\beta}(r, t) = A_{\alpha\beta} e^{i\vec{k}\cdot\vec{r}} e^{-i\omega t}. \quad (4.7)$$

Here the requirement of being Hermitian  $A_{\alpha\beta} = A_{\beta\alpha}^*$ .

In our description of the system with the density matrix, we will not use the full quantum mechanical density matrix, but treat the space and momentum degrees of freedom semiclassically in order to understand the real space behavior better. Internal degrees of freedom will, however, be treated quantum mechanically. We define a semiclassical density matrix  $\varrho(r, p)$ , and an internal density matrix  $\rho(r)$  as,

$$\begin{aligned} \varrho_{\alpha\beta}(r, p) &= \int d^3r' \langle \psi_{\alpha}^{\dagger}(r + \frac{r'}{2}) \psi_{\beta}(r - \frac{r'}{2}) \rangle e^{i\vec{p}\cdot\vec{r}'}, \\ \rho_{\alpha\beta}(r) &= \int \frac{d^3p}{(2\pi)^3} \varrho_{\alpha\beta}(r, p) = \langle \psi_{\alpha}^{\dagger}(r) \psi_{\beta}(r) \rangle. \end{aligned} \quad (4.8)$$

The diagonal matrix elements of the internal density matrix  $\rho_{\alpha\alpha}(r)$  give the density of particles in the internal state  $\alpha$  at point  $r$ . The off-diagonal elements measure the coherence between the internal states [11].



We can derive an equation of motion for  $\varrho(r, p)$ , by starting with the Heisenberg equations of motion for the field operator,

$$\frac{d}{dt}\psi_\alpha(r) = i[\mathcal{H}, \psi_\alpha(r)], \quad (4.9)$$

and taking the expectation values to get  $\frac{d\varrho}{dt}(r, p)$ . The contribution of each term in the Hamiltonian to the evolution of  $\varrho(r, p)$  can be calculated separately. As an example, we present the calculation of the potential energy contribution:

$$\begin{aligned} \dot{\psi}_\alpha(r) &= i \left[ \int d^3 r' \sum_\gamma U_\gamma(r') \psi_\gamma^+(r') \psi_\gamma(r'), \psi_\alpha(r) \right] \\ &= i \int d^3 r' \sum_\gamma U_\gamma(r') [\psi_\gamma^+(r'), \psi_\alpha(r)] \psi_\gamma^+(r') \\ &= -i U_\alpha(r) \psi_\alpha(r). \end{aligned} \quad (4.10)$$

Upon complex conjugation one obtains

$$\dot{\psi}_\alpha^+(r) = i U_\alpha(r) \psi_\alpha^+(r). \quad (4.11)$$

Now one can write the contribution of potential energy to  $\frac{d\varrho}{dt}(r, p)$  as follows:

$$\begin{aligned} \dot{\varrho}_{\alpha\beta}^{(\text{Pot})}(r, p) &= \int d^3 r' e^{ip \cdot r'} \left( \langle \dot{\psi}_\alpha^+(r + r'/2) \psi_\beta(r - r'/2) \rangle + \langle \psi_\alpha^+(r + r'/2) \dot{\psi}_\beta(r - r'/2) \rangle \right) \\ &\simeq i \int d^3 r' e^{ip \cdot r'} \left( U_\alpha(r) - U_\beta(r) + \vec{r}' \cdot \nabla_r \left( \frac{U_\alpha(r) + U_\beta(r)}{2} \right) \right) \langle \psi_\alpha^+(r + r'/2) \psi_\beta(r - r'/2) \rangle \\ &= i(U_\alpha(r) - U_\beta(r)) \varrho_{\alpha\beta}(r, p) + \nabla_r \left( \frac{U_\alpha(r) + U_\beta(r)}{2} \right) \cdot \nabla_p \varrho_{\alpha\beta}(r, p). \end{aligned} \quad (4.12)$$

Going through this procedure for each of the terms in the Hamiltonian (4.4), one arrives the equation of motion. In that calculation whenever we need to find an expectation value of a four-particle operator we use Wick's theorem,

$$\langle \psi_\alpha^+ \psi_\beta^+ \psi_\beta \psi_\alpha \rangle = \langle \psi_\alpha^+ \psi_\alpha \rangle \langle \psi_\beta^+ \psi_\beta \rangle + \langle \psi_\alpha^+ \psi_\beta \rangle \langle \psi_\beta^+ \psi_\alpha \rangle. \quad (4.13)$$

In the averaging (4.13), the first term represents direct (Hartree) contribution and cor-

responds to forward scattering. The second term is the exchange (Fock) contribution and is related to the backward scattering. Note that this term involves off-diagonal rather than diagonal components of the density matrix.

Putting everything together we find the following equation for the space and time variation of the density matrix:

$$\begin{aligned}
& \left( \partial_t + \frac{\vec{p}}{m} \cdot \nabla_r - \nabla_r \left( \frac{U_\alpha(r) + U_\beta(r)}{2} \right) \cdot \nabla_p \right) \varrho_{\alpha\beta}(r, p) \\
&= i \left[ U_\alpha(r) - U_\beta(r) + \sum_\gamma (\lambda_{\gamma\alpha} - \lambda_{\gamma\beta}) \rho_{\gamma\gamma}(r) \right] \varrho_{\alpha\beta}(r, p) \\
&+ i \sum_\gamma \lambda_{\gamma\alpha} \rho_{\alpha\gamma}(r) \varrho_{\gamma\beta}(r, p) - i \sum_\gamma \lambda_{\beta\gamma} \rho_{\gamma\beta}(r) \varrho_{\alpha\gamma}(r, p) \\
&+ \sum_\gamma \frac{\lambda_{\gamma\alpha} + \lambda_{\beta\gamma}}{2} \nabla_r \rho_{\gamma\gamma}(r) \cdot \nabla_p \varrho_{\alpha\beta}(r, p) \\
&+ \sum_\gamma \frac{\lambda_{\gamma\alpha}}{2} \nabla_r \rho_{\alpha\gamma}(r) \cdot \nabla_p \varrho_{\gamma\beta}(r, p) - \sum_\gamma \frac{\lambda_{\beta\gamma}}{2} \nabla_r \rho_{\gamma\beta}(r) \cdot \nabla_p \varrho_{\alpha\gamma}(r, p) \\
&+ i \sum_\gamma [A_{\gamma\alpha}(r, t) \varrho_{\gamma\beta}(r, p) - A_{\beta\gamma}(r, t) \varrho_{\alpha\gamma}(r, p)] \\
&+ \frac{1}{2} \sum_\gamma [\nabla_r A_{\gamma\alpha}(r, t) \cdot \nabla_p \varrho_{\gamma\beta}(r, p) - \nabla_r A_{\beta\gamma}(r, t) \cdot \nabla_p \varrho_{\alpha\gamma}(r, p)].
\end{aligned} \tag{4.14}$$

Now we recall the assumptions made in chapter 3, and use them to simplify this general equation. We assume a homogeneous system, and thus set  $U_\alpha(r) = \hbar\omega_\alpha$ . We also assume a weak external excitation field, which implies that the components of the density matrix involving state 2 are small:

$$\varrho_{11} \simeq n \gg \varrho_{12}, \varrho_{22}. \tag{4.15}$$

We can then consider transport equations for  $\varrho_{11}$  and  $\varrho_{12}$  separately. For  $\varrho_{11}$ , neglecting terms of order  $(\varrho_{12})^2$ ,  $(\varrho_{22})^2$ , Eq.(4.14) gives

$$\left( \partial_t + \frac{\vec{p}}{m} \cdot \nabla_r \right) \varrho_{11}(r, p) = 0. \tag{4.16}$$

This equation is equivalent to the continuity equation. For  $\varrho_{12}$  we have

$$\begin{aligned} (\partial_t + \frac{\vec{p}}{m} \cdot \nabla_r) \varrho_{12}(r, p) = & i [\omega_{12} + (\lambda_{11} - \lambda_{12})\rho_{11}] \varrho_{12}(r, p) \\ & + i \lambda_{11} \rho_{11}(r) \varrho_{12}(r, p) - i \lambda_{21} \rho_{12}(r) \varrho_{11}(r, p). \end{aligned} \quad (4.17)$$

Going to a Fourier transform representation by

$$\varrho_{12}(r, p, t) = \varrho_{12}(p) e^{i(\vec{k} \cdot \vec{r} - \omega t)}, \quad (4.18)$$

we obtain an integral equation of the form

$$\left[ \omega - \frac{\vec{p}}{m} \cdot \vec{k} - \omega_{21} + (2\lambda_{11} - \lambda_{12})n \right] \varrho_{12}(p) = \lambda_{12} \varrho_{11}(p) \int \frac{d^3 p'}{(2\pi)^3} \varrho_{12}(p'). \quad (4.19)$$

When this equation is solved by iteration, it gives an expression proportional to the response function  $\Pi(k, \omega)$ , calculated in the Chapter 3. This after all is not too surprising when we investigate the right hand side of the Kubo formula expression for the response function in Eq.(2.20). The response function is proportional to the amplitude of oscillation of the off-diagonal part of the density matrix.

We have therefore found the quantity constituting the collective mode –the coherence between the states 1 and 2 that forms the “wave” we are looking for. Although it seems to be somewhat more abstract than, for instance density waves forming sound, we see that this collective mode is measurable. Another way to understand this mode is to make an analogy with a spin problem. One can think of state 1 and state 2 as representing the spin up and spin down states of some fictitious spin, then the collective mode would be the oscillations of the transverse ( $x - y$ ) components of this spin.

An important point to note about the transport equation (4.14) is that it does not include a collision integral. The processes we are interested in happen at much shorter time-scales than the ordinary elastic collisions, because the collective mode is formed as a result of coherent evolution. Such collective modes are called collisionless collective modes, other better known examples being the zero sound in Fermi liquids,

or first and second sound in Bose-Einstein condensates [1, 39].

If the collision integral were included in the transport equation, its main effect would have been a weak damping of the collective mode. This effect was accounted for, by adding the diagram in Fig.(3-1 j) to the calculation in the previous chapter.

Here we would like to emphasize that the optical collective mode we have discussed is similar in many ways to zero sound in Fermi liquids. Both of them are collisionless collective modes, which arise from the evolution of a particle-hole pair. The two important differences are the particle statistics and the difference of the internal states of the particle and the hole for the optical collective mode. Still, the physical pictures given for zero sound[39] are most of the time relevant for the optical modes considered .

We now discuss how this collective mode manifests itself in the lineshape found as a result of the calculations in the Chapter 3. We first look at the average density shift.

We have found that for an interacting system, the optical resonance at  $\omega_0$  is shifted to the frequency

$$\omega = \omega_0 + 2(\lambda_{12} - \lambda_{11})n, \quad (4.20)$$

for a spatially homogeneous excitation. The magnitude of the shift (4.20) would be difficult to understand in terms of the individual shifts of the one particle internal states 1 and 2. Attempting this, one would have to say that the shifted energy level for state 1 is given by

$$\omega_1 \rightarrow \omega_1 - 2\lambda_{11}n, \quad (4.21)$$

where the factor of two arises from Bose statistics. For state 2, the same logic would lead one to the mean density shift

$$\omega_2 \rightarrow \omega_2 - \lambda_{12}n, \quad (4.22)$$

and the difference of these two shifts is a result different from Eq(4.20) by the amount of  $\lambda_{12}n$ . This is the effect of the collective mode, and we need a more careful analysis

to understand it.

To this end, consider a gas of  $n$  particles, all in the 1<sup>st</sup> internal state, in a box of unit volume with periodic boundary conditions. Let  $|0\rangle$  denote a (properly symmetrized) state in which the momentum states  $k_1, k_2, k_3, \dots$  are filled, and there are no particles in internal state 2

$$|0\rangle = |k_1, k_2, k_3, \dots\rangle \otimes |0\rangle. \quad (4.23)$$

We can see that upon the action of the excitation Hamiltonian with  $k = 0$ , the new state will be in a manifold spanned by states which have one of the momentum states  $k_1, k_2, k_3, \dots$  filled by a particle in internal state 2.

$$\begin{aligned} |1\rangle &= |k_2, k_3, k_4, \dots\rangle \otimes |k_1\rangle \\ |2\rangle &= |k_1, k_3, k_4, \dots\rangle \otimes |k_2\rangle \\ &\vdots \\ &\vdots \\ &\vdots \end{aligned} \quad (4.24)$$

The energy difference between these states and  $|0\rangle$  is precisely the incorrect shift obtained in the one particle picture

$$\langle m|\mathcal{H}|m\rangle - \langle 0|\mathcal{H}|0\rangle = \omega_0 + (\lambda_{12} - 2\lambda_{11})n. \quad (4.25)$$

However, none of the states  $|m\rangle$  are eigenstates of the interaction Hamiltonian. In fact, for any  $0 < l, m \leq n$ , we have,

$$\langle m|\mathcal{H}|n\rangle = \lambda_{12}. \quad (4.26)$$

When we diagonalize the Hamiltonian (4.4) in the subspace, the result is very interesting. All but one of the eigenstates  $|v_1\rangle, \dots, |v_{n-1}\rangle$ , have the same energy as  $|m\rangle$ . The only state which has a different energy is the symmetric combination of  $|1\rangle, \dots, |n\rangle$

$$|sym\rangle = \frac{1}{\sqrt{n}} (|1\rangle + |2\rangle + \dots + |n\rangle), \quad (4.27)$$

with the energy being,

$$\langle sym|\mathcal{H}|sym\rangle - \langle 0|\mathcal{H}|0\rangle = \omega_0 + 2(\lambda_{12} - \lambda_{11})n. \quad (4.28)$$

One may be lead to think that as only one state out of many has this energy, it will hardly show up in the optical spectrum. However, it is exactly the opposite. The symmetric state is the only state that contributes to the optical spectrum. The reason is that all other eigenstates in the subspace have zero overlap with the excitation operator:

$$\langle v_i|\mathcal{H}_{exc}|0\rangle = 0. \quad (4.29)$$

Thus, the only state that is excited is the symmetric state (4.28). This state has an important property that not only is it invariant under the exchange of two particles in state 1, it is also invariant under the exchange of the particle in the second internal state with any of the particles in state 1. One can see that the excitation Hamiltonian acts only to change the internal state wavefunction, but leaves the spatial wavefunction intact. Thus, all the spatial correlations of the initial particle are transferred to the excited particle.

Generalizing this further, one notes that, since the spatial wavefunction of the excited particle does not change through the excitation process, the spatial part of the many body wavefunction must be invariant under the exchange of the particle that goes through the excitation with any of the particles in the gas, in state 1 or state 2. This viewpoint leads us to generalize our result to initial states with particles in state 2 present. In this case, the optical mode resonance is at,

$$\omega = \omega_0 + 2(\lambda_{12} - \lambda_{11})n_1 + 2(\lambda_{22} - \lambda_{12})n_2. \quad (4.30)$$

We will derive this result in Chapter 6, from the transport equation.

Now we attempt to understand the other properties of the lineshape in terms of our physical picture of the optical collective mode as oscillations of the off-diagonal

part of the density matrix. We have derived the dispersion relation,

$$\omega_k = \omega_0 + 2(\lambda_{12} - \lambda_{11})n + \frac{\hbar^2 k^2}{2m} + \frac{v_T^2 k^2}{3\lambda_{12}n}. \quad (4.31)$$

We explained the second term of (4.31) in terms of exchange interaction of Bosons above, and the first and third terms do not need any explanation. Let us try to interpret the last term.

In the transport equation, we have our optical mode at  $\omega, k$  represented by,

$$\varrho_{12}(r, p, t) = \varrho_{12}(p)e^{i(\vec{k}\cdot\vec{r}-\omega t)}, \quad (4.32)$$

which satisfies Eq.(4.19) for each  $\omega, k$ . Thus the momentum distribution of the optical mode  $\varrho_{12}(p)$ , depends on wavevector  $k$  of the excitation field. Therefore, the interaction energy of the excitation depends on how  $\rho_{12}$  is distributed over the momentum states. Thus the source of the last term is the dependence of the interaction energy on the momentum distribution  $\varrho_{12}(p)$  of the optical mode.

Since the collective mode has a non-zero frequency at  $k = 0$ , we expect the dispersion relation to have a smooth derivative at this point. Also, the isotropy of the space requires  $\vec{k}$  and  $-\vec{k}$  to have the same  $\omega$  value. The smallest power of  $k$  satisfying this requirement is 2, explaining the  $k^2$  dependence. The origin of the factor of 1/3 is the angular average of the term  $(\vec{k} \cdot \vec{p})^2$ , as seen in the derivation Eq.(3.39).

Another important feature of the lineshape is the narrowing of the linewidth with increasing gas density. One might expect increasing density to broaden the line, as it increases the number of collisions. However, it is known that if the collisions do not effect the coherence of the optical process, and trap the particle to less than a wavelength of the excitation field, we expect a narrowing of the line. This effect is the well known Dicke narrowing. We have demonstrated that the exchange collisions which change the momentum of the state 2 particle and the state 1 hole, are fully coherent. Let us estimate the length scale that they confine this pair. Roughly, this length scale is of the order of the distance traversed in the time between two exchange

collisions,

$$l_{coh} \sim \tau_{coh} v_T \simeq \frac{v_T}{\lambda_{12} n}. \quad (4.33)$$

Thus, the criterion for narrowing is,

$$l_{coh} \ll \frac{2\pi}{k}, \quad (4.34)$$

which gives us,

$$k v_T \ll \lambda_{12} n. \quad (4.35)$$

Eq.(4.35) shows that when  $k$  is small enough for the collective mode to be well defined, the narrowing effect takes place.

We must, however, make it clear that the effect in our case, although analogous, is not equivalent to Dicke narrowing. The narrowing effect is not due to the localization of the particle in the excited state, but due to the localization of the coherence  $\varrho_{12}(\tau)$  in space. In other words, the density modes  $\varrho_{11}$  and  $\varrho_{12}$  behave diffusively with a diffusion constant related to  $\tau_{el}$  and not  $\tau_{coh}$ . Thus, the behavior of  $\varrho_{22}$  and  $\varrho_{12}$  are radically different, the first being a diffusive mode, while the other is a reactive (massive) mode with an imaginary diffusion constant. If we imagine the optical excitation to be localized initially, we would see the density mode to diffuse away from the localization region, while the coherence mode will go through many cycles of oscillation in the envelope provided by the density mode, expanding much more slowly.

Now, we want to extend the picture we have given so far, to the case of a condensed gas. When the condensate forms, a finite fraction of the particles occupy the ground state, and the first term of the sum in the expression for the density matrix Eq.(2.12) becomes as important as the sum of the rest. Thus, when we need to describe the state of the gas in the semi-classical approximation, we need not only keep track of the semiclassical density matrix  $\varrho_{\alpha\beta}(r, p, t)$ , but also of the vector of condensate wavefunctions in each internal state  $\bar{\psi}_\alpha$ .



This can be achieved in second quantization by replacing the field operators by

$$\hat{\psi}_\alpha(r) \rightarrow \hat{\psi}_\alpha(r) + \bar{\psi}_\alpha(r), \quad (4.36)$$

where  $\bar{\psi}_\alpha$  is not an operator but a complex number representing the condensate wavefunction [3]. Although the dynamics of the condensate can be described by specifying a vector of complex numbers at each point, we find it useful to use a matrix representation for this vector,

$$\bar{\rho}_{\alpha\beta}(r) = \bar{\psi}_\alpha^*(r)\bar{\psi}_\beta(r). \quad (4.37)$$

We should emphasize that this matrix is always of rank one, and so it does not contain any more information than  $\bar{\psi}_\alpha$ , but it is introduced only for convenience. We also need to keep track of the condensate flows,

$$\vec{J}_{\alpha\beta}(r) = i\frac{\hbar}{2m} \left[ (\nabla\bar{\psi}_\alpha^*(r))\bar{\psi}_\beta(r) - \bar{\psi}_\alpha^*(r)(\nabla\bar{\psi}_\beta(r)) \right]. \quad (4.38)$$

Finally, for deriving the coupled equations of motion for  $\varrho$  and  $\bar{\rho}$  we use

$$\frac{d}{dt}\bar{\psi}_\alpha(r) = -i\frac{\partial\mathcal{H}}{\partial\bar{\psi}_\alpha^*(r)}, \quad (4.39)$$

the Heisenberg equation for the classical field  $\bar{\psi}_\alpha$ . The equation of motion for  $\bar{\rho}$  can be obtained similar methods used in the derivation of the equation for  $\varrho$  (4.14). We find that the coupled behavior of these two matrices are governed by the equations,

$$\begin{aligned} & \left( \partial_t + \frac{\vec{p}}{m} \cdot \nabla_r - \nabla_r \left( \frac{U_\alpha(r) + U_\beta(r)}{2} \right) \cdot \nabla_p \right) \varrho_{\alpha\beta}(r, p) \\ &= i \left[ U_\alpha(r) - U_\beta(r) + \sum_\gamma (\lambda_{\gamma\alpha} - \lambda_{\gamma\beta}) \rho_{\gamma\gamma}^{\text{tot}}(r) \right] \varrho_{\alpha\beta}(r, p) \\ &+ i \sum_\gamma \lambda_{\gamma\alpha} \rho_{\alpha\gamma}^{\text{tot}}(r) \varrho_{\gamma\beta}(r, p) - i \sum_\gamma \lambda_{\beta\gamma} \rho_{\gamma\beta}^{\text{tot}}(r) \varrho_{\alpha\gamma}(r, p) \\ &+ \sum_\gamma \frac{\lambda_{\gamma\alpha} + \lambda_{\beta\gamma}}{2} \nabla_r \rho_{\gamma\gamma}^{\text{tot}}(r) \cdot \nabla_p \varrho_{\alpha\beta}(r, p) \end{aligned} \quad (4.40)$$

$$\begin{aligned}
& + \sum_{\gamma} \frac{\lambda_{\gamma\alpha}}{2} \nabla_r \rho_{\alpha\gamma}^{\text{tot}}(r) \cdot \nabla_p \varrho_{\gamma\beta}(r, p) - \sum_{\gamma} \frac{\lambda_{\beta\gamma}}{2} \nabla_r \rho_{\gamma\beta}^{\text{tot}}(r) \cdot \nabla_p \varrho_{\alpha\gamma}(r, p) \\
& + i \sum_{\gamma} [V_{\gamma\alpha}(r, t) \varrho_{\gamma\beta}(r, p) - V_{\beta\gamma}(r, t) \varrho_{\alpha\gamma}(r, p)] \\
& + \frac{1}{2} \sum_{\gamma} [\nabla_r V_{\gamma\alpha}(r, t) \cdot \nabla_p \varrho_{\gamma\beta}(r, p) - \nabla_r V_{\beta\gamma}(r, t) \cdot \nabla_p \varrho_{\alpha\gamma}(r, p)]
\end{aligned}$$

and

$$\begin{aligned}
& \left( \partial_t \bar{\rho}_{\alpha\beta}(r) + \nabla_r \cdot \vec{J}_{\alpha\beta}(r) \right) \tag{4.41} \\
& = i \left[ U_{\alpha}(r) - U_{\beta}(r) + \sum_{\gamma} (\lambda_{\gamma\alpha} - \lambda_{\gamma\beta}) \rho_{\gamma\gamma}^{\text{tot}}(r) \right] \bar{\rho}_{\alpha\beta}(r) \\
& + i \left[ \sum_{\gamma} \lambda_{\gamma\alpha} \rho_{\alpha\gamma}(r) \bar{\rho}_{\gamma\beta}(r) - \sum_{\gamma} \lambda_{\beta\gamma} \rho_{\gamma\beta}(r) \bar{\rho}_{\alpha\gamma}(r) \right] \\
& + i \sum_{\gamma} [V_{\gamma\alpha}(r, t) \bar{\rho}_{\gamma\beta}(r) - V_{\beta\gamma}(r, t) \bar{\rho}_{\alpha\gamma}(r)]
\end{aligned}$$

where  $\rho^{\text{tot}}(r) = \rho(r) + \bar{\rho}(r)$ .

We now expect, much like the quantity  $\varrho_{12}$  which is related to the optical response of the normal gas, the evolution of  $\bar{\rho}_{12}$  to define the optical response of the condensate. The physical picture we have for  $\bar{\rho}_{12}$  is much simpler than that for  $\varrho_{12}$ . Consider changing the internal state of one of the atoms in the condensate from state 1 to state 2. The excited atom in a different internal state from all the other atoms in the condensate, will still share their spatial wavefunction. However the state 2 atom does not go through exchange scatterings, and thus the extra  $\lambda_{12}n$  frequency shift is absent for a condensate mode,

$$\omega = \omega_0 + (\lambda_{12} - 2\lambda_{11})n. \tag{4.42}$$

However, the actual answer is not as simple as two separate modes, associated with normal gas and condensate, oscillating at different frequencies. After simplifying the transport equations (4.40),(4.41) for uniform density, and assuming the density in

state 1 to be much higher than in state 2,

$$\rho_{11} \gg \rho_{12}, \rho_{22}; \quad \bar{\rho}_{11} \gg \bar{\rho}_{12}, \bar{\rho}_{22}, \quad (4.43)$$

we arrive at the coupled equations.

$$\frac{d}{dt} \begin{bmatrix} \rho_{12} \\ \bar{\rho}_{12} \end{bmatrix} = \begin{bmatrix} \omega_0 + (2\lambda_{11} - \lambda_{12})n + \lambda_{11}n_c & \lambda_{12}n_c \\ \lambda_{12}n_T & \omega_0 + (2\lambda_{11} - \lambda_{12})n - \lambda_{11}n_c \end{bmatrix} \begin{bmatrix} \rho_{12} \\ \bar{\rho}_{12} \end{bmatrix}. \quad (4.44)$$

The mechanism for the coupling in (4.44) is again exchange collisions. For instance, one can have a state 2 particle with momentum  $k$  making an exchange collision with a particle in the condensate. As a result, the state 1 particle in the condensate will go to the momentum state  $k$ , while the state 2 particle will acquire the condensate wavefunction. The reverse process is also possible. One can have a state 2 particle in the condensate excited to a momentum state  $k$ , through an exchange collision with a state 1 particle in this state. The rates of such processes are clearly proportional to the condensate density  $n_c$ , and the thermal density  $n_T$ , respectively. Technically, these processes are represented as the off-diagonal elements in Eq.(4.44).

The eigenvalues of the matrix in Eq.(4.44), are the resonance frequencies for the normal peak and the condensate peak, as found in the previous chapter. Investigating the eigenvectors of the problem (4.44) provides additional insight about the system. First, we see that except when  $n_c = 0$ , the two modes are always coupled, and thus the eigenvectors are neither purely normal, nor purely condensed modes as discussed earlier. Each optical eigenmode has both components.

When we are at the transition temperature  $T = T_c$ , the condensate density is very close to zero and the modes are basically uncoupled. Then the normal gas resonance frequency is characterized by a  $2\lambda_{12}n$  shift, while the condensate resonance shift is  $\lambda_{12}n$ . As the temperature is lowered, coupling becomes significant. Initially, like two quantum states which are mixed, the frequencies of the two modes repel each other. There is, however, another effect which becomes important at lower temperatures. As  $T \rightarrow 0$ , condensate density  $n_c$  becomes much greater than normal density  $n_T$ , and

for both of the eigenmodes, condensate contribution becomes much more important compared to that of the normal part. When  $T$  is very close to 0, both of the modes are predominantly condensate modes, and their frequencies approach each other. At zero temperature, there is no difference between the two modes, and they merge at,

$$\omega = \omega_0 - (2\lambda_{11} - \lambda_{12})n. \quad (4.45)$$

The observed doubling of the number of collective modes upon Bose condensation is not unexpected. Once a finite fraction of particles start to occupy the same state, the wavefunction of this state can be treated as a classical field, with its own excitations, and these excitations by the definition of the condensate, are collective. The phenomenon of second sound in superfluid  $^4\text{He}$  and Alkali Bose condensates is another example which demonstrates a similar doubling of collective modes.

To conclude, in this chapter we have presented another, more intuitive approach to the theory for collective optical excitations, both below and above Bose condensation. We demonstrated how the coherent processes, forward and exchange scattering, effect the internal dynamics of the gas, and how they couple the optical modes in the condensate and the normal gas.

## Chapter 5

# A Sum Rule for the Cold Collision Frequency Shift

All the discussion that we have presented thus far about the interaction effects on the optical spectrum has been based on a perturbative expansion in the strength of interactions. Although this is an excellent approximation for dilute systems under consideration, some features in the resulting lineshape follow from the basic symmetries of the system, and are free of any errors that are introduced by making this approximation.

Unfortunately, it is very hard to extend the above calculation to a system which has a spatially varying external potential. Despite that we will show that the effects of this external potential on some general properties of the lineshape are easily calculable.

In this chapter, we will be concerned with one such property of the lineshape, the average frequency shift of the spectrum defined as,

$$\bar{\omega} = \frac{\int d\omega \omega \mathcal{I}(\omega)}{\int d\omega \mathcal{I}(\omega)}. \quad (5.1)$$

We have already obtained an expression for the average frequency shift, by using the lineshape calculated in perturbation theory in Chapter 3. We will now show that the average frequency shift can be obtained without calculating the lineshape explicitly.

This can be accomplished even in the presence of an external potential, which, we will show does not affect the result directly.

We start by writing the Hamiltonian in real space,

$$\begin{aligned}
\mathcal{H} &= \mathcal{H}_0 + \mathcal{H}_{int}, \\
\mathcal{H}_0 &= \int d^3r \sum_{\alpha=1,2} \psi_{\alpha}^{\dagger}(r) \left( -\frac{\hbar^2 \nabla^2}{2m} + \hbar U_{\alpha}(r) \right) \psi_{\alpha}(r), \\
\mathcal{H}_{int} &= \int d^3r \sum_{\alpha,\beta=1,2} \frac{\hbar \lambda_{\alpha\beta}}{2} \psi_{\alpha}^{\dagger}(r) \psi_{\beta}^{\dagger}(r) \psi_{\beta}(r) \psi_{\alpha}(r),
\end{aligned} \tag{5.2}$$

where, as in the previous chapter,  $U_{\alpha}(r)$  the external potential coupling to the atoms in the internal state  $\alpha$  includes the internal energies  $\hbar\omega_{\alpha}$ . The transitions between the internal states are facilitated by the external field,

$$\mathcal{H}_{exc} = \int d^3r A_{12}(r) e^{-i\omega t} \psi_{\alpha}^{\dagger}(r) \psi_{\beta}(r) + h.c. \tag{5.3}$$

Now, we return to the Kubo formula expression for the lineshape we have obtained in Chapter 2, Eq.(2.20). By introducing a set of complete states and carrying out the time integration explicitly, we write it in the form,

$$\mathcal{I}(\omega) = \frac{2\pi}{\hbar} \sum_{n,m} \delta(\hbar\omega + \epsilon_n - \epsilon_m) |\langle m | \mathcal{H}_{exc} | n \rangle|^2 p_n, \tag{5.4}$$

where  $p_n$  is the probability distribution for the many body state  $n$  in our ensemble. For a system in thermal equilibrium  $p_n$  is the Boltzmann factor. In this form, we see that the Kubo formula is equivalent to the Fermi's golden rule for transition probabilities between many body states.

We now continue with the evaluation of the average density shift by considering the numerator and the denominator separately. For the numerator, after carrying out the  $\omega$  integration, we have

$$\int \frac{d\omega}{2\pi} \omega \mathcal{I}(\omega) = \frac{1}{\hbar^2} \sum_{n,m} (\omega_m - \omega_n) |\langle m | \mathcal{H}_{exc} | n \rangle|^2 p_n \tag{5.5}$$

$$\begin{aligned}
&= \frac{1}{\hbar^3} \sum_{n,m} \langle n | \mathcal{H}_{\text{exc}} | m \rangle \langle m | [\mathcal{H}, \mathcal{H}_{\text{exc}}] | n \rangle p_n \\
&= \langle \mathcal{H}_{\text{exc}} [\mathcal{H}, \mathcal{H}_{\text{exc}}] \rangle,
\end{aligned}$$

where the averaging in the last term is understood as an ensemble average  $\sum_n \langle n | \cdots | n \rangle p_n = \langle \cdots \rangle$ .

We can now consider the commutator of each term in the Hamiltonian individually. The first feature to notice is that the spatially varying part of the potential,  $\int d^3r U(r) \sum_{\alpha} \psi_{\alpha}^{\dagger} \psi_{\alpha}$ , commutes with  $\mathcal{H}_{\text{exc}}$ , and thus does not affect the end result directly. Because this potential determines the density distribution in the first place, its effects will be seen in the average frequency indirectly. However, once the density distribution is known, in order to find the average frequency shift, it is not important to know the exact form of the external potential resulting in this distribution.

For the remaining two terms in the Hamiltonian, we can calculate the contributions to the numerator separately,

$$\int \frac{d\omega}{2\pi} \omega \mathcal{I}(\omega) = F_{kin} + F_{int}, \quad (5.6)$$

where the first term is the contribution of kinetic energy in the Hamiltonian, and the second one is due to the interparticle interaction.

We first calculate the contribution of the kinetic energy. In this calculation, we proceed by using the bosonic commutation relations,

$$[\psi_{\alpha}(r), \psi_{\beta}^{\dagger}(r')] = \delta_{\alpha\beta} \delta(r - r'), \quad (5.7)$$

to put the expressions into normal order by placing all the annihilation operators to the right of creation operators. Then, recalling the assumption that there are no particles in state 2 initially, we use

$$\psi_2(r) |n\rangle = 0, \quad (5.8)$$

for all  $n$ . We obtain

$$F_{kin} = \int \frac{d^3r}{\hbar^3} (\lambda_{11} - \lambda_{12}) |A(r)|^2 \langle \psi_1^+(r) \psi_1^+(r) \psi_1(r) \psi_1(r) \rangle. \quad (5.9)$$

The expression to be averaged is familiar as the two point correlation function at zero separation  $g_2$ ,

$$\langle \psi_1^+(r) \psi_1^+(r) \psi_1(r) \psi_1(r) \rangle = g_2(r) n^2(r). \quad (5.10)$$

Thus, we have the result,

$$F_{int} = \int \frac{d^3r}{\hbar^3} (\lambda_{11} - \lambda_{12}) |A(r)|^2 g_2(r) n^2(r). \quad (5.11)$$

In calculating the contribution of kinetic energy, we follow the same procedure. The commutator gives us

$$-\frac{\hbar^2}{2m} \langle \int \frac{d^3r}{\hbar^3} \psi_1^+(r) A^*(r) [\nabla^2, A(r)] \psi_1(r) \rangle. \quad (5.12)$$

We can now express the external field in terms of its magnitude and phase as,

$$A(r) = |A(r)| e^{i\theta(r)}, \quad (5.13)$$

and integrate Eq.(5.12) by parts to obtain

$$\begin{aligned} F_{kin} &= \int d^3r \frac{\hbar^2}{2m} [\nabla |A(r)| + |A(r)| \nabla \theta(r)] e^{i\theta(r)} n(r) \\ &- \int \frac{d^3r}{2m} \hbar |A(r)|^2 \vec{j}(r) \cdot \vec{\nabla} \theta(r), \end{aligned} \quad (5.14)$$

where the local density and particle flux are given by

$$n(r) = \langle \psi_1^+(r) \psi_1(r) \rangle, \quad \vec{j}(r) = -\frac{i\hbar}{2m} \langle \psi_1^+(r) \vec{\nabla} \psi_1(r) \rangle + h.c. \quad (5.15)$$

We need to calculate the denominator to complete the calculation of the average



density shift. By normal ordering the state 2 operators, we easily get

$$\int \frac{d\omega}{2\pi} \mathcal{I}(\omega) = \int d^3r \hbar^3 |A(r)|^2 n(r). \quad (5.16)$$

Finally we have

$$\bar{\omega} - \omega_0 = \frac{\int d^3r \left[ (\lambda_{12} - \lambda_{11}) g_2(r) n^2(r) |A(r)|^2 + \frac{\hbar^2}{2m} (\nabla A(r))^2 n(r) - \hbar |A|^2 \vec{j} \cdot \vec{\nabla} \theta \right]}{\int d^3r |A(r)|^2 n(r)} \quad (5.17)$$

We can now analyze the terms inside the numerator. The first term, which is the interaction contribution, is the only term which is non-zero when the excitation is uniform,  $A(r) = A$ . We have studied this case in detail in the previous chapter, and it is in accordance with our picture of “inherited correlation” that the interaction shifts depend on the two point correlation function of the gas composed of only state 1 particles, not that of a gas having one state 2 particle in it.

The kinetic terms can be understood as the generalizations of the recoil shift and Doppler shift to the non-homogeneous density and excitation. If we take the excitation field to be  $A = A_0 e^{i\vec{k} \cdot \vec{r}}$ , these two terms give us,

$$|A_0|^2 \int \frac{d^3r}{\hbar^3} \left( \frac{\hbar^2 k^2}{2m} - \hbar \frac{\vec{k} \cdot \vec{j}}{m} \right) n, \quad (5.18)$$

which are the usual expressions for recoil and Doppler shifts. We see that the relative importance of the kinetic and interaction contributions can be judged by looking at the average wavevector of the excitation, and comparing  $\hbar^2 k^2 / (2m)$  with  $(\lambda_{12} - \lambda_{11})n$ , provided that there are no macroscopic flows in the gas.

We must remark here that the sum rule implies nothing about the broadening of the spectrum, which may result from the distribution of interactions shifts, Doppler broadening, or the interaction broadening via ordinary elastic collisions. The expression for the average shift given here is, however, correct regardless of how broad the spectrum is.

It is also clear that the average frequency shift does not depend on the power of

the excitation field, as long as it is weak. We have obtained this expression in the linear response regime, and both the numerator and the denominator are first order in  $|A(r)|^2$ . Again, this linear response approximation allows us to get two separate contributions, one solely due to interactions, the other due to kinetic effects. Non-linear effects will be considered in the next chapter.

The presented form of the sum rule is just an exact identity relating the average frequency shift to the two point correlation function  $g_2(r)$ , the density distribution  $n(r)$ , the current distribution  $\vec{j}(r)$ , and the excitation field  $A(r)$ . As long as these quantities are known, the shift is determined, regardless of whether the gas is not in equilibrium or in an external potential. Still, in order to apply the sum rule to any experimental situation these quantities, if not directly measured, must be calculated within some approximation about thermal equilibrium, density distribution, etc. [41]

We can investigate the average frequency shift for a homogeneous system with no permanent currents under a harmonic excitation field. We get

$$\bar{\omega} - \omega_0 = (\lambda_{12} - \lambda_{11})g_2n + \frac{\hbar^2 k^2}{2m}. \quad (5.19)$$

It is well known that for temperatures above Bose condensation temperature,

$$g_2 = 2, \quad (5.20)$$

and for temperatures below condensation,

$$g_2 = 2 - \frac{n_c^2}{n^2}. \quad (5.21)$$

Thus, the sum rule results in the same expression obtained with the perturbative treatment of the previous chapters. This shows us that the main physical principles underlying the sum rule are preserved in our perturbation treatment.

We can list three physical principles that together form the basis for the sum rule. The first is that the total number of particles is conserved locally. The second is that spatial correlations before excitation takes place are transferred to the excited

particle. And the third is the Bosonic symmetry of the many body wavefunction under exchange.

We can say that the first principle is mainly responsible for the kinetic terms, while the second and the third combine to give us the interaction term. We can make an interesting connection to the well known f-sum rule [40] for the structure factor by considering the following limit .

If we take the interactions between two particles in different states to be the same as the interactions between two particles in the same internal state and take  $\omega_0$  to zero, we eliminate all the difference between the internal states. In this case, our sum rule reduces to the f-sum rule. In the center of mass frame, for a harmonic excitation, we get from Eq.(5.17),

$$\int \frac{d\omega}{2\pi} \mathcal{I}(\omega, k) = |A_0|^2 \frac{\hbar^2 k^2}{2m} \int d^3r n(r), \quad (5.22)$$

which is the f-sum rule.

Our excitation Hamiltonian works both in the Hilbert space of internal states by changing the internal states of the particles, and also in the external (real) space by giving an extra momentum to the particles. Due to the assumed weakness of the excitation Hamiltonian, we can separate its action on these two spaces to find the interaction and kinetic contributions to the average density shift. When  $k = 0$ , we have the excitation Hamiltonian acting only in the internal space and obtain the interaction density shift, while for  $\lambda_{12} = \lambda_{11}$ , and  $\omega_0 = 0$ , we get the familiar f-sum rule for the density response.

With the derivation of the sum rule, we conclude our exploration of the linear response regime of the optical excitations. In the next chapter, we will consider the effect of a strong excitation field on the optical modes, and investigate the resulting non-linear effects using the sum rule.

# Chapter 6

## Nonlinear Optical Response

Up to this point, we have only considered situations in which the excitation field causing the optical excitations is weak. We have assumed that the number of particles going through an internal state transition is much smaller than the total density. However, experiments have been carried out on dilute atomic gases in which an important fraction or all of the particles change their internal states [18, 19, 30, 22]. The existence of such experiments raises the need to investigate the physics of optical excitations away from the linear response regime.

In this chapter, we will extend the theory developed so far to explain the effects of coherent collisions on the internal state transitions, to the strong excitation regime. Here, the internal states of the particles are coupled to the excitation field strongly, and the dynamics is more complicated than the linear response case.

Our starting point for the investigation of this regime will be the coupled transport equations we derived for the normal and condensate density matrices in Eq.(4.40), which we reproduce here,

$$\begin{aligned} & \left( \partial_t + \frac{\vec{p}}{m} \cdot \nabla_r - \nabla_r \left( \frac{U_\alpha(r) + U_\beta(r)}{2} \right) \cdot \nabla_p \right) \varrho_{\alpha\beta}(r, p) \\ & = i \left[ U_\alpha(r) - U_\beta(r) + \sum_\gamma (\lambda_{\gamma\alpha} - \lambda_{\gamma\beta}) \rho_{\gamma\gamma}^{\text{tot}}(r) \right] \varrho_{\alpha\beta}(r, p) \\ & + i \sum_\gamma \lambda_{\gamma\alpha} \rho_{\alpha\gamma}^{\text{tot}}(r) \varrho_{\gamma\beta}(r, p) - i \sum_\gamma \lambda_{\beta\gamma} \rho_{\gamma\beta}^{\text{tot}}(r) \varrho_{\alpha\gamma}(r, p) \end{aligned} \quad (6.1)$$

$$\begin{aligned}
& + \sum_{\gamma} \frac{\lambda_{\gamma\alpha} + \lambda_{\beta\gamma}}{2} \nabla_r \rho_{\gamma\gamma}^{\text{tot}}(r) \cdot \nabla_p \varrho_{\alpha\beta}(r, p) \\
& + \sum_{\gamma} \frac{\lambda_{\gamma\alpha}}{2} \nabla_r \rho_{\alpha\gamma}^{\text{tot}}(r) \cdot \nabla_p \varrho_{\gamma\beta}(r, p) - \sum_{\gamma} \frac{\lambda_{\beta\gamma}}{2} \nabla_r \rho_{\gamma\beta}^{\text{tot}}(r) \cdot \nabla_p \varrho_{\alpha\gamma}(r, p) \\
& + i \sum_{\gamma} [V_{\gamma\alpha}(r, t) \varrho_{\gamma\beta}(r, p) - V_{\beta\gamma}(r, t) \varrho_{\alpha\gamma}(r, p)] \\
& + \frac{1}{2} \sum_{\gamma} [\nabla_r V_{\gamma\alpha}(r, t) \cdot \nabla_p \varrho_{\gamma\beta}(r, p) - \nabla_r V_{\beta\gamma}(r, t) \cdot \nabla_p \varrho_{\alpha\gamma}(r, p)],
\end{aligned}$$

and

$$\begin{aligned}
& (\partial_t \bar{\rho}_{\alpha\beta}(r) + \nabla_r \cdot \vec{J}_{\alpha\beta}(r)) = \\
& + i \left[ U_{\alpha}(r) - U_{\beta}(r) + \sum_{\gamma} (\lambda_{\gamma\alpha} - \lambda_{\gamma\beta}) \rho_{\gamma\gamma}^{\text{tot}}(r) \right] \bar{\rho}_{\alpha\beta}(r) \\
& + i \left[ \sum_{\gamma} \lambda_{\gamma\alpha} \rho_{\alpha\gamma}(r) \bar{\rho}_{\gamma\beta}(r) - \sum_{\gamma} \lambda_{\beta\gamma} \rho_{\gamma\beta}(r) \bar{\rho}_{\alpha\gamma}(r) \right] \\
& + i \sum_{\gamma} [V_{\gamma\alpha}(r, t) \bar{\rho}_{\gamma\beta}(r) - V_{\beta\gamma}(r, t) \bar{\rho}_{\alpha\gamma}(r)],
\end{aligned} \tag{6.2}$$

where  $\rho^{\text{tot}}(r) = \rho(r) + \bar{\rho}(r)$ .

Our main interest in this chapter will be the consequences of interparticle interactions in the internal state dynamics, so we will simplify the above general equations by assuming that we are in a uniform system, with no normal or condensate flows, and further assume that the external fields are applied uniformly. With these assumptions, there is no further need for the full density matrix  $\varrho(r, p)$ , as the internal dynamics is completely described by  $\rho(r)$ , which will be the same for all points  $r$ . Thus, equations of motion reduce to

$$\begin{aligned}
\dot{\rho}_{\gamma\gamma'} & = i (w_{\gamma} - w_{\gamma'} + U_{\gamma} - U_{\gamma'}) \rho_{\gamma\gamma'} + i \sum_{\alpha} \lambda_{\alpha\gamma} (\rho_{\gamma\alpha} + \bar{\rho}_{\gamma\alpha}) \rho_{\alpha\gamma'} \\
& - i \sum_{\alpha} \lambda_{\alpha\gamma'} (\rho_{\alpha\gamma'} + \bar{\rho}_{\alpha\gamma'}) \rho_{\gamma\alpha} + i \sum_{\alpha} (V_{\alpha\gamma}(t) \rho_{\alpha\gamma'} - V_{\gamma'\alpha}(t) \rho_{\gamma\alpha}),
\end{aligned} \tag{6.3}$$

$$\begin{aligned}
\dot{\bar{\rho}}_{\gamma\gamma'} & = i (w_{\gamma} - w_{\gamma'} + U_{\gamma} - U_{\gamma'}) \bar{\rho}_{\gamma\gamma'} + i \sum_{\alpha} \lambda_{\alpha\gamma} \rho_{\gamma\alpha} \bar{\rho}_{\alpha\gamma'} \\
& - i \sum_{\alpha} \lambda_{\alpha\gamma'} \rho_{\alpha\gamma'} \bar{\rho}_{\gamma\alpha} + i \sum_{\alpha} (V_{\alpha\gamma}(t) \bar{\rho}_{\alpha\gamma'} - V_{\gamma'\alpha}(t) \bar{\rho}_{\gamma\alpha}),
\end{aligned} \tag{6.4}$$

where  $U_\gamma$  are defined as,

$$\sum_{\beta} \lambda_{\alpha\beta} (\rho_{\beta\beta} + \bar{\rho}_{\beta\beta}) U_{\alpha} = \sum_{\beta} \lambda_{\alpha\beta} n_{\beta}. \quad (6.5)$$

The dynamics described in the above equations are fairly complicated if there are fields coupling more than two states, so we will concentrate on the simplest case, where only two internal states are coupled, and all the populations in the other states remain constant. Then we will be concerned with the dynamics of two,  $2 \times 2$  matrices, one for the normal gas, and one for the condensate. If we assume that states 1 and 2 are coupled, we can go to a Larmor basis with the frequency of the coupling field, so that the elements of our density matrix (and similarly the condensate matrix) can be redefined. The diagonal elements of the matrices do not change, while the off-diagonal elements change as

$$\rho'_{12} = \rho_{12} \exp[-i\Omega_{12}t], \quad \rho'_{21} = (\rho'_{12})^*. \quad (6.6)$$

In this basis we will find it useful to rewrite the equations of motion in the Bloch representation [11]. We can expand these  $2 \times 2$  Hermitian matrices as,

$$\begin{aligned} \rho'_{\gamma\gamma'} &= \rho_0 \delta_{\gamma\gamma'} + \vec{S} \cdot \vec{\sigma}_{\gamma\gamma'} \\ \bar{\rho}'_{\gamma\gamma'} &= \bar{\rho}_0 \delta_{\gamma\gamma'} + \vec{S}_c \cdot \vec{\sigma}_{\gamma\gamma'}, \end{aligned} \quad (6.7)$$

where  $\vec{\sigma}$  are the Pauli matrices.

In this representation,  $\bar{\rho}_0$  and  $\rho_0$  will be proportional to the total number of atoms in the condensate, and above the condensate, respectively. The  $z$ -components of both spins are proportional to the population difference between the internal states, belonging to the normal gas or the condensate. For the normal part, the norm of the projection of spin onto the  $x - y$  plane represents the degree of coherence between the two internal states. For the condensate spin, however, this norm is directly proportional to the geometric mean of the populations of the two internal states. Furthermore for both cases, the angle corresponding to a rotation around the  $z$  axis

is related to the relative phase of the two internal states.

The matrix  $V_{\alpha\beta}$  has no diagonal elements, as defined in the excitation Hamiltonian. However, we can take the detunings that come as a result of going to Larmor basis as the diagonal elements,  $V_{11}(V_{22})$  being defined as  $+(-)[w_2 - w_1 - \Omega_{12}]$ . We then can again expand  $V_{\gamma\gamma'}$  as,

$$V_{\gamma\gamma'} = V_0\delta_{\gamma\gamma'} + \vec{V} \cdot \vec{\sigma}_{\gamma'\gamma}. \quad (6.8)$$

In this representation, we can write the equations of motion for the condensate and the normal gas spins as :

$$\begin{aligned} \dot{\vec{S}} &= \vec{S} \times \vec{B}_n + 2\lambda_{12}\vec{S} \times \vec{S}_c + 2\vec{S} \times \vec{V} \\ \dot{\vec{S}}_c &= \vec{S}_c \times \vec{B}_c + 2\lambda_{12}\vec{S}_c \times \vec{S} + 2\vec{S}_c \times \vec{V}, \end{aligned} \quad (6.9)$$

with

$$\begin{aligned} \vec{B}_n &= [(\lambda_{11} - \lambda_{22})(2\rho_0 + \bar{\rho}_0) + (\lambda_{11} + \lambda_{22} - 2\lambda_{12})(2\vec{S} + \vec{S}_c) \cdot \hat{z}]\hat{z} \\ \vec{B}_c &= [(\lambda_{11} - \lambda_{22})(\rho_0 + \bar{\rho}_0) + (\lambda_{11} + \lambda_{22} - 2\lambda_{12})(\vec{S} + \vec{S}_c) \cdot \hat{z}]\hat{z}. \end{aligned} \quad (6.10)$$

It is important to observe that the equations conserve the total densities in the condensed and non condensed fractions of the gas. To make a better sense of the equations, we can note that they can be derived from the XXZ self interacting Hamiltonian,

$$\begin{aligned} \mathcal{H} = & (\lambda_{11} - \lambda_{22})(\rho_0 + \bar{\rho}_0)\hat{z} \cdot (\vec{S} + \vec{S}_c) + (\lambda_{11} - \lambda_{22})\rho_0\hat{z} \cdot \vec{S} \\ & + J^{ij}S^iS^j + \frac{1}{2}J^{ij}S_c^iS_c^j + J^{ij}S_c^iS^j \\ & + 2(\vec{S} + \vec{S}_c) \cdot \vec{V}, \end{aligned} \quad (6.11)$$

where

$$J = \begin{pmatrix} 2\lambda_{12} & 0 & 0 \\ 0 & 2\lambda_{12} & 0 \\ 0 & 0 & (\lambda_{11} + \lambda_{22}) \end{pmatrix}, \quad (6.12)$$

using the Poisson spin algebra,

$$\begin{aligned} \{S^i, S^j\} &= \epsilon^{ijk} S^k \\ \{S_c^i, S_c^j\} &= \epsilon^{ijk} S_c^k \\ \{S^i, S_c^j\} &= 0. \end{aligned} \quad (6.13)$$

## 6.1 The Single Spin Problem

We start the analysis of the dynamics described in Eq.(6.9) by considering the situation in which we can represent the system by a single spin. There are two such cases. The first one is at zero temperature, when almost all the atoms are in the condensate, while the second is above the transition temperature, when there is no condensate present. However, our analysis is still restricted to temperatures low enough to satisfy the quantum gas condition,  $\lambda_T > a_s$  of Eq.(1.3).

We first analyze equations of motion Eq.(6.9) for the case where there is no external field. Such an analysis is needed to understand any interaction related effects in experiments where particles spend a substantial amount of time in a superposition state, such as in atomic clocks [16, 30, 22, 15].

We first consider the case where there is no Bose condensation. Our equations (6.9) will then be reduced to

$$\dot{\vec{S}} = \vec{S} \times \vec{B}_n. \quad (6.14)$$

We can easily see that the  $z$ -component of spin will be conserved, and we will only have a precession around the  $z$  axis with a precession frequency

$$\omega = (w_2 - w_1) + 2(\lambda_{22}n_2 - \lambda_{11}n_1 + \lambda_{12}(n_1 - n_2)) + \sum_{\gamma \neq 1,2} (\lambda_{2\gamma} - \lambda_{1\gamma})n_\gamma. \quad (6.15)$$



This result agrees with the theory of frequency shifts in atomic clocks [25, 48, 47].

We can now ask the same question for a sample which is fully condensed. When all the atoms are in the condensate, they will all be sharing the same spatial wavefunction, and this will indicate that no exchange processes will be possible. That would eliminate the factor of 2 multiplying the combination of  $\lambda$  and  $n$ 's for states 1 and 2 in Eq.(6.15). Not surprisingly, for a fully condensed sample, we get

$$\omega = (w_2 - w_1) + (\lambda_{22}n_2 - \lambda_{11}n_1 + \lambda_{12}(n_1 - n_2)) + \sum_{\gamma \neq 1,2} (\lambda_{2\gamma} - \lambda_{1\gamma})n_\gamma. \quad (6.16)$$

In the presence of an external field, the populations in the internal states will change according to Eq.(6.9). Recall that, these equations are derived in a frame rotating at the angular frequency of the external field, and any apparent detuning fields resulting from the difference between the external field frequency and natural transition frequency are absorbed into the external field vector  $\vec{V}$ .

In this section, we consider the response to an external field, only when the system can be represented by a single spin, that is, the system is either fully condensed or not condensed at all. In the latter case, we have the equation,

$$\begin{aligned} \dot{\vec{S}} &= \vec{S} \times \vec{B}_n + 2\vec{S} \times \vec{V} \\ \vec{B}_n &= [(\lambda_{11} - \lambda_{22})2\rho_0 + (\lambda_{11} + \lambda_{22} - 2\lambda_{12})2\vec{S} \cdot \hat{z}]\hat{z}. \end{aligned} \quad (6.17)$$

The former case has similar equations with  $S_c$  replacing  $S$  and  $B_c$  being half of  $B_n$ .

Since the dynamics conserves the magnitude of the spin, we only have two dynamical variables, which can be taken as angles  $(\theta, \phi)$  in the spherical polar coordinates, representing the orientation of the spin. Another conserved quantity in this dynamics is the Hamiltonian introduced earlier,

$$\begin{aligned} \mathcal{H} = & (\lambda_{11} - \lambda_{22})\rho_0\hat{z} \cdot \vec{S} + (\lambda_{11} - \lambda_{22})\rho_0\hat{z} \cdot \vec{S} \\ & + J^{ij}S^iS^j + 2\vec{S} \cdot \vec{V}. \end{aligned} \quad (6.18)$$

On the sphere defined by  $(\theta, \phi)$ , contours of constant  $\mathcal{H}$  will define the paths

along which the spin will precess. We can treat both the normal gas case and the fully condensed case by writing the Hamiltonian as a function of  $(\theta, \phi)$  as

$$\mathcal{H} = A \cos^2(\theta) + B \cos(\theta) + C \sin(\theta) \cos(\phi) + D, \quad (6.19)$$

and identify

$$\begin{aligned} A &= \frac{1}{2}(\lambda_{11} + \lambda_{22} - 2\lambda_{12})|S_c|^2, \\ B &= ((\lambda_{11} - \lambda_{22})\bar{\rho}_0|S_c| + 2V^z|S_c|), \\ C &= 2V^x|S_c|, \\ D &= \lambda_{12}|S_c|^2, \end{aligned} \quad (6.20)$$

for the fully condensed case, and

$$\begin{aligned} A &= (\lambda_{11} + \lambda_{22} - 2\lambda_{12})|S|^2, \\ B &= (2(\lambda_{11} - \lambda_{22})\rho_0|S| + 2V^z|S|), \\ C &= 2V^x|S|, \\ D &= 2\lambda_{12}|S|^2, \end{aligned} \quad (6.21)$$

for the normal gas.

In the presence of strong external fields the paths are almost circular with centers on the line oriented along vector  $\vec{V}$ , passing through the origin, as in the usual Rabi problem, and significant changes in the populations occur throughout the course of a Rabi oscillation. As a function of  $\theta$  and  $\phi$ , the Hamiltonian has one maximum and one minimum. All the trajectories circle these extremum points, if the external field satisfies

$$\left| \frac{C}{A} \right| > \left( 1 - \left| \frac{B}{A} \right|^{2/3} \right)^{3/2}. \quad (6.22)$$

When the intrinsic Rabi frequency  $|\vec{V}|$ , becomes of the order of the density caused shifts ( $\sim \lambda n$ ), an interesting situation occurs. Even on resonance, large population transfers from one state to another does not take place. This can be easily seen from

the structure of trajectories on the Bloch sphere. When the external field does not satisfy Eq.(6.22), instead of having one minimum and one maximum, the Hamiltonian has two maxima, one minimum and a saddle point. The two constant  $\mathcal{H}$  trajectories crossing at the saddle point separate the sphere into three regions, giving us three kinds of trajectories, circling the minimum or one of the two maxima. None of these oscillations, however, result in large population transfers, which is in contrast with the Rabi problem. In the Rabi problem one can change internal states of all the atoms with an arbitrarily small field on resonance. This effect can be understood if we realize that the transition frequency for an atom depends on the populations. So for weak fields, even a small population transfer carries the transition away from resonance, *i.e.*, makes the effective detuning much larger than the Rabi frequency.

In both cases, we can calculate the oscillation frequency along each path. The period of the precession along a path  $\mathcal{C}$  on which  $\mathcal{H}(\theta, \phi) = \mathcal{H}'$  is given by

$$T(\mathcal{H}') = \int_{\mathcal{C}} dl \frac{1}{|\nabla \mathcal{H}|}. \quad (6.23)$$

By converting the integral to a surface integral over a  $\delta$  function, and integrating over the angle  $\phi$ , we have

$$T = \frac{2}{|A|} \int dx \frac{1}{\sqrt{x^4 + C_3 x^3 + C_2 x^2 + C_1 x + C_0}}, \quad (6.24)$$

where,

$$\begin{aligned} C_3 &= 2\frac{B}{A}, \\ C_2 &= \left( \frac{C^2 + B^2}{A^2} - 2\frac{H - D}{A} \right), \\ C_1 &= -2\frac{B(H - D)}{A^2}, \\ C_0 &= -\frac{C^2 - (H - D)^2}{A^2}. \end{aligned} \quad (6.25)$$

In the high field case, for the external field satisfying Eq.(6.22), the Hamiltonian will take values between  $H_{max}$  and  $H_{min}$ , the values of the Hamiltonian at the max-

imum and minimum points, respectively. Any value of  $H$  in this range will uniquely correspond to one trajectory, and the period of motion on such a trajectory will be given by,

$$\begin{aligned} T &= \frac{4}{|A|\sqrt{pq}} K\left(\frac{1}{2}\sqrt{\frac{(x_1 - x_2)^2 - (p - q)^2}{pq}}\right), \\ p^2 &= (m - x_1)^2 + n^2, \\ q^2 &= (m - x_2)^2 + n^2, \end{aligned} \quad (6.26)$$

where  $K$  is the complete elliptic integral [5],  $x_1, x_2$  are the real roots,  $m$  is the real part and  $n$  is the absolute value of the imaginary part of the remaining two complex conjugate roots of the polynomial in Eq.(6.24).

In the weak field case, there are four special values of the Hamiltonian, the minimum value  $\mathcal{H}_{min}$ , the value at the saddle point  $\mathcal{H}_{saddle}$ , the smaller and the larger of the values at the two maxima  $\mathcal{H}_{max<}$  and  $\mathcal{H}_{max>}$  (See Fig. contourlines). For  $\mathcal{H}$  values in the range  $\mathcal{H}_{max>} > \mathcal{H}' > \mathcal{H}_{max<}$  or  $\mathcal{H}_{saddle} > \mathcal{H} > \mathcal{H}_{min}$  there is again one to one correspondence between  $\mathcal{H}$  values and trajectories on the sphere. For such trajectories the frequencies are again given by (6.26). For the values of  $H$  satisfying  $\mathcal{H}_{max<} > \mathcal{H} > \mathcal{H}_{saddle}$  there are two trajectories corresponding to each  $\mathcal{H}$ , one circling  $\mathcal{H}_{max<}$ , and the other circling  $\mathcal{H}_{max>}$ . However, they both have the same period given by

$$T = \frac{4}{|A|\sqrt{(x_4 - x_2)(x_3 - x_1)}} K\left(\sqrt{\frac{(x_2 - x_1)(x_4 - x_3)}{(x_4 - x_2)(x_3 - x_1)}}\right), \quad (6.27)$$

where  $K$  is again the complete elliptic integral, and  $x_1 < x_2 < x_3 < x_4$  are the four real roots of the polynomial in Eq.(6.24).

A typical plot of frequencies for the weak field case is given in Fig.(6-2). Near the saddle point trajectories, the logarithmic slow-down in  $\mathcal{H} - \mathcal{H}_{saddle}$  is as expected from the two dimensional dynamics.

When we use these equations to describe a fully condensed sample, the cases of low field and high field behavior correspond to two well known phenomena, Rabi oscillations [11] and internal Josephson oscillations [51]. We can also see that for a

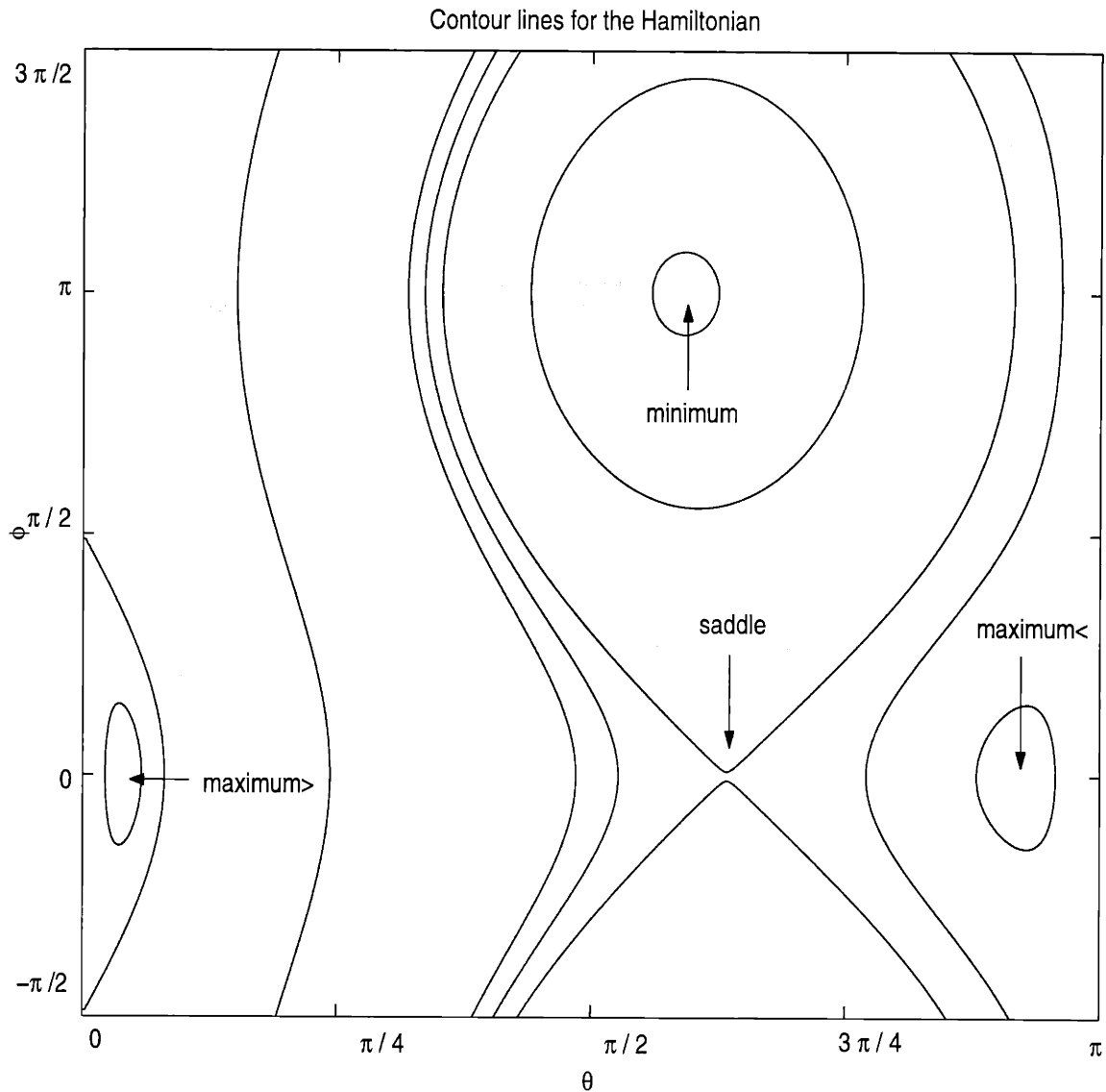


Figure 6-1: The contour lines for the Hamiltonian Eq.(6.19), on the Bloch sphere, defined by  $\theta$ ,  $\phi$ , for weak external fields. As the field strength is increased, the saddle point comes closer to one of the maxima and they destroy each other when the condition in Eq.(6.22) is satisfied, leaving just one maximum and one minimum. In the figure the trajectories encircling the maxima correspond to Josephson oscillations with an average phase difference of  $\pi$ , while those encircling the minimum are the usual Josephson oscillations corresponding to small oscillations of phase difference. The frequencies of motion along these trajectories are given in Fig.(6-2).

condensate, our equations reduce to those obtained in [50, 45] by using two coupled Gross-Pitaevskii equations. At high field, we get almost circular trajectories, and correspondingly large oscillations between internal levels of the condensate, as in the Rabi problem. For the low field case, we get three kinds of trajectories all of which give little population change, corresponding to Josephson oscillations. Two of these three kinds of trajectories complete a full cycle around the  $z$ -axis, while the third is trapped in a region for which  $\phi_{min} < \phi < \phi_{max}$ . Recalling that  $\phi$  represents the relative phase of the two condensates, we see that these trajectories correspond to Josephson oscillations between the two internal states, caused by the weak link of the external field. The other two kinds of trajectories again correspond to Josephson oscillations. However, in this class of Josephson oscillations there is a  $2\pi$  phase slip for every period of population change.

From the above discussion we can come to the conclusion that to observe the internal Josephson effect, it is not required to have two Bose condensed samples, although two words of caution should be voiced about this. First we have only considered the coherent collisions, and the coherence of the phase of two internal levels will be destroyed on a time scale that is set by mean free time in the gas. Any observed internal Josephson oscillation should decay in this time scale. Second, to be able to see this effect one has to go to very low field strengths, so that the population oscillations should be observable in a non-condensed sample.

Still, we have shown that it is not absolutely necessary to have Bose condensation to observe small oscillations in the relative phase of the internal states under a small excitation field. We can imagine a non-condensed gas of atoms put into a superposition of two internal states by a  $\pi/2$  pulse. If this sample is further subjected to weak mixing field on resonance, one would naively expect population transfer from one internal level to the other with the Rabi frequency of the field. However, our discussion shows that if the sample and the field satisfy

$$\tau_{\text{free}}^{-1} = 8\pi a_s^2 n v_T \ll |\vec{V}| \ll \lambda n, \quad (6.28)$$

we would have small oscillations of the phase and populations, which is exactly what is observed in the internal Josephson effect with condensed samples.

## 6.2 The Two Spin Problem

After analyzing the fully condensed and non-condensed Bose gases, both of which can be represented by only one spin in our Eqs. (6.9), we turn our attention to the partially condensed Bose gas. When the temperature is between zero and condensation temperature,  $T_c$ , both condensed and non-condensed densities are present. If these densities are comparable, we have to use the full form of Eq.(6.9), with both spins present.

We first start with the free precession problem, by setting the external field equal to zero. In this case, we have the equations,

$$\dot{\vec{S}} = \vec{S} \times \vec{B}_n + 2\lambda_{12}\vec{S} \times \vec{S}_c \quad (6.29)$$

$$\dot{\vec{S}}_c = \vec{S}_c \times \vec{B}_c + 2\lambda_{12}\vec{S}_c \times \vec{S}. \quad (6.30)$$

The effective magnetic fields  $\vec{B}_n$  and  $\vec{B}_c$  both point in the  $\hat{z}$  direction and are defined in Eq.(6.10). Since their time derivatives are perpendicular to the spin vectors, norm of both of the spins,  $|\vec{S}|$  and  $|\vec{S}_c|$  are conserved. This conservation simply means that the total number of atoms in the condensate and over the condensate are conserved. Another conserved quantity can be obtained by adding Eq.(6.29) to Eq.(6.30), and taking the  $\hat{z}$  component. We have,

$$\frac{d}{dt} \left( \hat{z} \cdot (\vec{S} + \vec{S}_c) \right) \equiv \frac{d}{dt} S_{\text{tot}}^z = 0. \quad (6.31)$$

Physically, this conservation law corresponds to the fact that in the absence of a coupling field, the total number of atoms in internal states 1 and 2 are conserved separately. Although these three conservation laws restrict the resulting dynamics considerably, they still allow oscillations in which the density of condensed and non-condensed atoms in internal state 1 change, while state 2 goes through the same

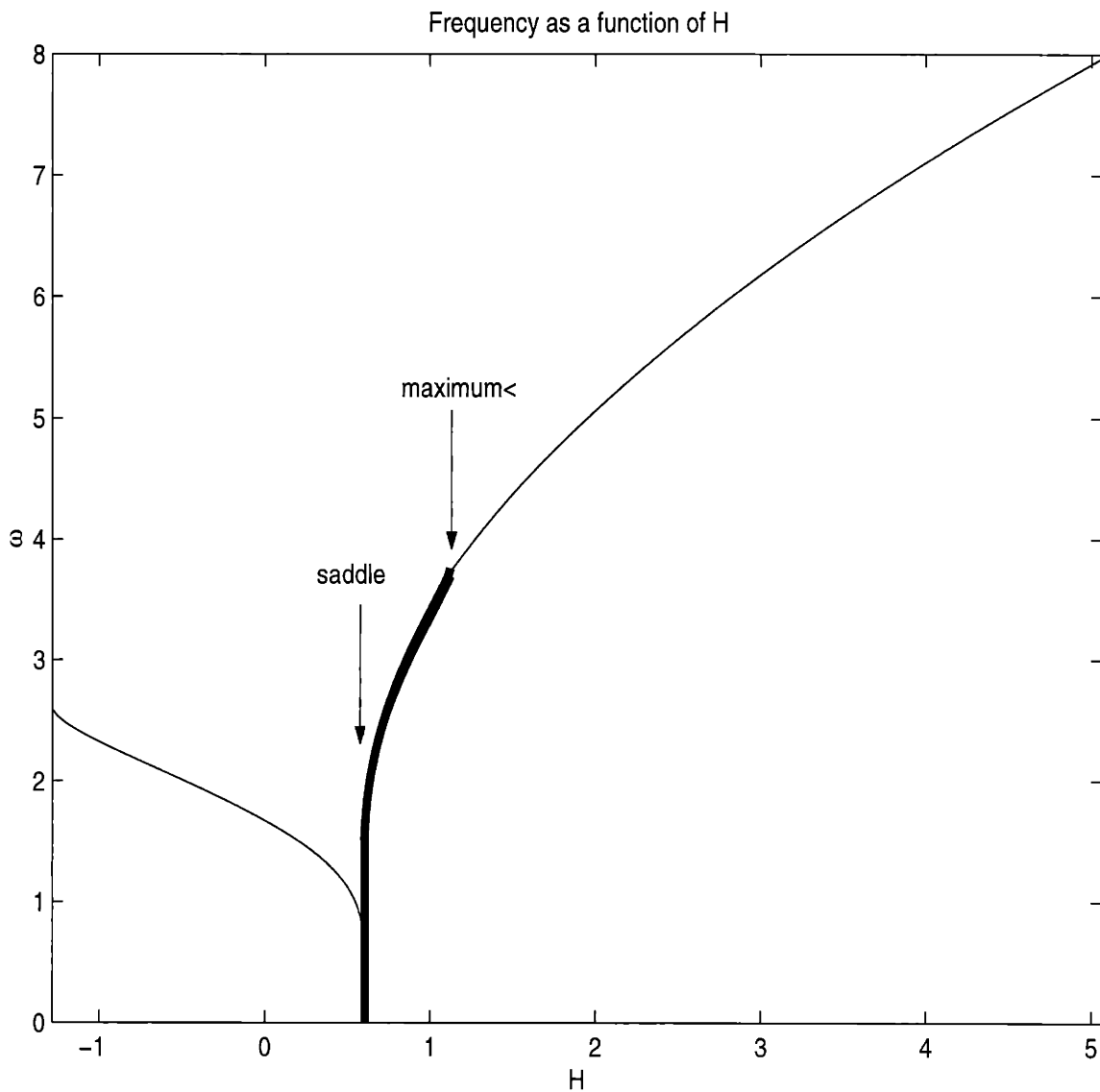


Figure 6-2: The frequency of precession on the Bloch sphere as a function of the value the Hamiltonian Eq.(6.19) takes. Hamiltonian can take values from  $H_{min}$  to  $H_{max}>$ . Near the saddle point the precession slows down logarithmically, as expected from a two dimensional dynamics. Between  $H_{saddle}$  and  $H_{max}>$  there are two trajectories for each value that the Hamiltonian takes. However, they both have the same frequency Eq.(6.27).



oscillations out of phase with state 1 keeping the total number of condensed and non-condensed atoms constant. In our spin representation, the degree of freedom that expresses these oscillations will be  $S^z$ , or equivalently  $S_c^z$ , as they add up to a constant.

The other conserved quantity is the Hamiltonian (6.11), which we now rewrite in terms of the conserved quantities  $S_{\text{tot}}^z$ ,  $|S|$ ,  $|S_c|$ , and the dynamical variable  $S^z$  as,

$$\begin{aligned} \mathcal{H} &= (\lambda_{11} - \lambda_{22})(\rho_0 + \bar{\rho}_0)S_{\text{tot}}^z + \frac{1}{2}(\lambda_{11} + \lambda_{22} - 2\lambda_{12})(S_{\text{tot}}^z)^2 \\ &+ 2\lambda_{12}|S|^2 + \lambda_{12}|S_c|^2 + (\lambda_{11} - \lambda_{22})\rho_0 S^z \\ &+ \frac{1}{2}(\lambda_{11} + \lambda_{22} - 2\lambda_{12})(S^z)^2 + 2\lambda_{12}\vec{S} \cdot \vec{S}_c. \end{aligned} \quad (6.32)$$

To look further into the oscillations of the degree of freedom physically described above and represented by  $S^z$  we take the equation of motion,

$$\frac{dS^z}{dt} = \hat{z} \cdot \dot{\vec{S}} = 2\lambda_{12}\hat{z} \cdot (\vec{S} \times \vec{S}_c) = 2\lambda_{12}\mathcal{V}. \quad (6.33)$$

Where  $\mathcal{V}$  is the volume of the parallelepiped formed by the vectors  $\hat{z}$ ,  $\vec{S}$  and  $\vec{S}_c$ . We can express the absolute value of this volume in terms of the inner products of these three vectors as

$$|\mathcal{V}| = \sqrt{|S|^2|S_c|^2 - (\vec{S} \cdot \vec{S}_c)^2 - |S_c|^2(S^z)^2 - |S|^2(S_c^z)^2 + 2S^z S_c^z \vec{S} \cdot \vec{S}_c}. \quad (6.34)$$

Now we can solve for  $\vec{S} \cdot \vec{S}_c$  in terms of conserved quantities and  $S^z$  from Eq.(6.32). This will give us the equation of motion for  $S^z$  expressed only in terms of conserved quantities and  $S^z$  itself,

$$\left| \frac{dS^z}{dt} \right| = \sqrt{C_4(S^z)^4 + C_3(S^z)^3 + C_2(S^z)^2 + C_1(S^z) + C_0} \quad (6.35)$$

The value of  $S^z$  will oscillate between  $x_1$  and  $x_2$ , which are the two roots of the polynomial inside the square root in Eq.(6.35). For values of  $S^z$  in the interval  $x_1 < S^z < x_2$ , this polynomial takes positive values. When  $S^z$  reaches its maximum

or minimum value, the vectors  $\vec{S}$ ,  $\vec{S}_c$  and  $\hat{z}$  are coplanar. This allows us to integrate Eq.(6.35) without paying attention to the absolute value. We can express the period of  $S^z$  as an integral of the form in Eq.(6.24),

$$T_z = 2 \int_{x_1}^{x_2} dS^z \frac{1}{\sqrt{C_4(S^z)^4 + C_3(S^z)^3 + C_2(S^z)^2 + C_1 S^z + C_0}}. \quad (6.36)$$

Due to the abundance of conserved quantities in the two spin problem, the expressions for the coefficients are more complicated compared to the one spin case,

$$\begin{aligned} C_4 &= -\frac{\Delta_2}{2} \left( \frac{\Delta_2}{2} - 4\lambda_{12} \right), \\ C_3 &= -[\Delta_1 \Delta_2 \rho_0 + 4\lambda_{12} \left( \frac{\Delta_2}{2} S_{\text{tot}}^z - \Delta_1 \rho_0 \right)], \\ C_2 &= [\Delta_2 (\mathcal{H} - \Delta_1 (\rho_0 + \bar{\rho}_0) S_{\text{tot}}^z - \frac{\Delta_2}{2} (S_{\text{tot}}^z)^2 - 2\lambda_{12} |S|^2 + \lambda_{12} |S_c|^2) \\ &\quad - 4\lambda_{12} (\mathcal{H} - \Delta_1 \bar{\rho}_0 S_{\text{tot}}^z - \frac{\Delta_2}{2} (S_{\text{tot}}^z)^2 + \lambda_{12} |S|^2)], \\ C_1 &= [(\mathcal{H} - \Delta_1 (\rho_0 + \bar{\rho}_0) S_{\text{tot}}^z - \frac{\Delta_2}{2} (S_{\text{tot}}^z)^2 - 2\lambda_{12} |S|^2 + \lambda_{12} |S_c|^2) (2\Delta_1 \rho_0 + 4\lambda_{12} S_{\text{tot}}^z) + 8\lambda_{12}^2 |S|^2 S_{\text{tot}}^z], \\ C_0 &= -(\mathcal{H} - \Delta_1 (\rho_0 + \bar{\rho}_0) S_{\text{tot}}^z - \frac{\Delta_2}{2} (S_{\text{tot}}^z)^2 - 2\lambda_{12} |S|^2 + \lambda_{12} |S_c|^2)^2 \\ &\quad + 2(\mathcal{H} - \Delta_1 (\rho_0 + \bar{\rho}_0) S_{\text{tot}}^z) (2\lambda_{12} |S|^2 + \lambda_{12} |S_c|^2) - 4\lambda_{12}^2 |S|^4 \\ &\quad - \lambda_{12}^2 |S_c|^4 - \Delta_2 \lambda_{12} |S_c|^2 (S_{\text{tot}}^z)^2 - 2(\Delta_2 + 2\lambda_{12}) \lambda_{12} |S|^2 (S_{\text{tot}}^z)^2, \end{aligned} \quad (6.37)$$

with the notation

$$\begin{aligned} \Delta_1 &= (\lambda_{11} - \lambda_{22}), \\ \Delta_2 &= (\lambda_{11} + \lambda_{22} - 2\lambda_{12}). \end{aligned} \quad (6.38)$$

As in the one spin case, this integral can be exactly evaluated [17]. If all the roots of the polynomial inside the square root in Eq.(6.35) are real, we have

$$T_z = \frac{4}{\sqrt{C_4}} \frac{1}{\sqrt{(x_4 - x_2)(x_3 - x_1)}} K \left( \sqrt{\frac{(x_2 - x_1)(x_4 - x_3)}{(x_4 - x_2)(x_3 - x_1)}} \right). \quad (6.39)$$

Here  $x_3 < x_4$  are the remaining real roots of the polynomial in the equation of motion

of Eq.(6.35), which are assumed to be real. In the case of imaginary  $x_3$  and  $x_4$ , an analogue of Eq.(6.26) will give the expression for the period.

The second oscillation for free precession corresponds to the precession of total phase about the  $z$ -axis. This precession is affected by the population oscillations found above, and the oscillation frequency is not as easily calculated. We can generally describe its motion as a sum of two components. The first one corresponds to a uniform precession around the  $z$ -axis with the density shift as in Eq(6.15), and the other corresponding to the effect of an oscillating magnetic field in  $\hat{z}$  direction, caused by the population oscillations discussed above. The coupling between these two components is best seen when we write the equation of motion for the spin components in the  $x - y$  plane. Defining  $S^+ = S^x + iS^y$ , and  $S_c^+ = S_c^x + iS_c^y$ , we have

$$\begin{aligned} i\dot{S}^+ &= (B_n(t) + 2\lambda_{12}S_c^z(t))S^+ - 2\lambda_{12}S^z(t)S_c^+ \\ i\dot{S}_c^+ &= -2\lambda_{12}S_c^z(t)S^+ + (B_c + 2\lambda_{12}S^z(t))S_c^+. \end{aligned} \quad (6.40)$$

We have seen that when  $S^z$  reaches its maximum or minimum values,  $\vec{S}$  and  $\vec{S}_c$  are in the same vertical plane. We can calculate exactly how much the spins have rotated around the  $z$ -axis throughout the course of one  $S^z$  oscillation. The effect of  $S^z$  oscillations will present itself through the integral,

$$I = \int_0^{T_z} dt S^z(t) = 2 \int_{x_1}^{x_2} \frac{S^z dS^z}{\left| \frac{dS^z}{dt} \right|} \quad (6.41)$$

which is again exactly calculable.

To calculate the rotation angle we integrate Eq.(6.40). After a time  $T_z$ ,  $S^+$  and  $S_c^+$  will be given by

$$\begin{bmatrix} S^+(T_z) \\ S_c^+(T_z) \end{bmatrix} = e^{i\mathcal{M}} \begin{bmatrix} S^+(0) \\ S_c^+(0) \end{bmatrix}, \quad (6.42)$$

where  $\mathcal{M}$  is a two by two matrix with elements

$$\mathcal{M}_{11} = \Delta_1(2\rho_0 + \bar{\rho}_0)T_z + (\Delta_2 + 2\lambda_{12})S_{\text{tot}}^z T_z + (\Delta_2 - 2\lambda_{12})I, \quad (6.43)$$

$$\begin{aligned}
\mathcal{M}_{12} &= -2\lambda_{12}I, \\
\mathcal{M}_{21} &= -2\lambda_{12}S_{\text{tot}}^z T_z + 2\lambda_{12}I, \\
\mathcal{M}_{22} &= \Delta_1(\rho_0 + \bar{\rho}_0)T_z + \Delta_2 S_{\text{tot}}^z T_z + 2\lambda_{12}.
\end{aligned}$$

Instead of giving the resulting long expression for the rotation angle in one period, we choose to describe the motion qualitatively. The precession of the two spins are affected by the competition between two effects. The first effect is, due to the absence of exchange scattering in the condensate, the condensate spin  $\vec{S}_c$  sees an effective magnetic field  $B_c$ , which is different from the effective magnetic field seen by the normal gas spin  $\vec{S}$ . The second one, as discussed above, is the condensate population oscillations characterized by  $S^z$ .

If there is not much difference between the densities of two internal states. Both spins lie close to the  $x - y$  plane, and their relative phase oscillates around zero, without ever growing large. However, if there is a lot of density difference between two internal states, the spins are close to the  $z$ -axis. Over one period of  $S^z$  oscillation, the phase difference can be a multiple of  $2\pi$ .

We can investigate the precession easily in the limit when both of the spins are almost aligned with the  $z$ -axis. We can write linear equations for the perpendicular components of the spins, and get the two precession frequencies,

$$\omega = \tilde{\omega} + (w_2 - w_1) + (U_2 - U_1 + \lambda_{22}n_2 - \lambda_{11}n_1) \quad (6.44)$$

with

$$\Delta n_{(c,t)} = n_{2(c,t)} - n_{1(c,t)}, \quad (6.45)$$

where  $\tilde{\omega}$  satisfies,

$$(\tilde{\omega} + \lambda_{12}\Delta n_t)(\tilde{\omega} - \lambda_{11}n_{c1} + \lambda_{22}n_{c2}) = \lambda_{12}^2 \Delta n_c \Delta n_t. \quad (6.46)$$

If the mixing angle is not small, in general one would expect to see two different frequencies. The average of the two frequencies will be controlled by the average

density shift seen by an atom in the sample, while the splitting will reflect the average rate the condensate fraction of one of the internal states oscillates [42].

The appearance of a second frequency should be detectable in an experiment that probes a partially condensed Bose gas in a superposition state. We propose using a partially condensed gas in a Ramsey separated field arrangement, as in the fountain atomic clocks [16, 30]. In this case the appearance of a second frequency would present itself as a beating in the Ramsey fringes. This beating, however, will vanish both in the limit of full condensation and in the limit of a normal gas, and should be most prominent when the condensate fraction is close to a half. The exact values of the frequencies can be obtained by solving the equations of motion Eq.(6.9) numerically.

Here we want to remind the reader that the equations used in this section Eq.(6.9) were derived for a uniform system. If the particles are cold enough, and the condensate is prepared in a shallow trap to make sure that the movement of each part of the cloud is negligible in the center of mass coordinate frame during the time of measurement, the equations will be locally correct and the experiment should show a density averaged result in the precession frequencies. Otherwise the effects of inhomogeneity must be included using the full transport equations of Eq.(6.1,6.2).

When an external field is turned on, the  $\hat{z}$  component of total spin is not conserved anymore, and there is a net population transfer from one internal state to the other. Much like the single spin case, we then have two limits. When  $|\vec{V}|$  is much larger than the density shift  $\lambda n$ , we have both spins following almost circular trajectories around  $\vec{V}$ . For the weak field case, the system can be best described as two non-linear oscillators going through coupled oscillations, with an occasional  $2\pi$  phase slip for one of them. In this most general case precession frequencies can be found by numerical integration of Eq.(6.9).

### 6.3 Fermions

Finally, to understand the effect of statistics better, we consider the same problem for a Fermi gas. We will have the same Hamiltonian as in Eq.(4.4), however, the

Fermionic field operators will satisfy

$$\{\psi_\alpha(r), \psi_\beta^\dagger(r')\} = \delta_{\alpha\beta}\delta(r - r'), \quad (6.47)$$

where  $\{, \}$  denotes the anti-commutator. The derivation will process along the same lines with the Bose case. The effect of statistics will be seen whenever we average a four particle operator. The exchange term in Eq.(4.13) will change sign,

$$\langle \psi_\alpha^\dagger \psi_\beta^\dagger \psi_\beta \psi_\alpha \rangle = \langle \psi_\alpha^\dagger \psi_\alpha \rangle \langle \psi_\beta^\dagger \psi_\beta \rangle - \langle \psi_\alpha^\dagger \psi_\beta \rangle \langle \psi_\beta^\dagger \psi_\alpha \rangle. \quad (6.48)$$

As a result, we get the transport equation for the density matrix defined as in Eq.(4.8), with sign changes in the terms corresponding to the exchange contributions,

$$\begin{aligned} & \left( \partial_t + \frac{\vec{p}}{m} \cdot \nabla_r - \nabla_r \left( \frac{U_\alpha(r) + U_\beta(r)}{2} \right) \cdot \nabla_p \right) \varrho_{\alpha\beta}(r, p) \\ &= i \left[ U_\alpha(r) - U_\beta(r) + \sum_\gamma (\lambda_{\gamma\alpha} - \lambda_{\gamma\beta}) \rho_{\gamma\gamma}(r) \right] \varrho_{\alpha\beta}(r, p) \\ & - i \sum_\gamma \lambda_{\gamma\alpha} \rho_{\alpha\gamma}(r) \varrho_{\gamma\beta}(r, p) + i \sum_\gamma \lambda_{\beta\gamma} \rho_{\gamma\beta}(r) \varrho_{\alpha\gamma}(r, p) \\ & + \sum_\gamma \frac{\lambda_{\gamma\alpha} + \lambda_{\beta\gamma}}{2} \nabla_r \rho_{\gamma\gamma}(r) \cdot \nabla_p \varrho_{\alpha\beta}(r, p) \\ & - \sum_\gamma \lambda_{\gamma\alpha} \nabla_r \rho_{\alpha\gamma}(r) \cdot \nabla_p \varrho_{\gamma\beta}(r, p) + \sum_\gamma \lambda_{\beta\gamma} \nabla_r \rho_{\gamma\beta}(r) \cdot \nabla_p \varrho_{\alpha\gamma}(r, p) \\ & + i \sum_\gamma [V_{\gamma\alpha}(r, t) \varrho_{\gamma\beta}(r, p) - V_{\beta\gamma}(r, t) \varrho_{\alpha\gamma}(r, p)] \\ & + \frac{1}{2} \sum_\gamma [\nabla_r V_{\gamma\alpha}(r, t) \cdot \nabla_p \varrho_{\gamma\beta}(r, p) - \nabla_r V_{\beta\gamma}(r, t) \cdot \nabla_p \varrho_{\alpha\gamma}(r, p)]. \end{aligned} \quad (6.49)$$

From the transport equation, by assuming all the interactions and the sample to be spatially homogeneous, we can get the equation of motion for the internal state density matrix,

$$\begin{aligned} \dot{\rho}_{\gamma\gamma'} &= i (w_\gamma - w_{\gamma'} + U_\gamma - U_{\gamma'}) \rho_{\gamma\gamma'} - i \sum_\alpha (\lambda_{\alpha\gamma} - \lambda_{\alpha\gamma'}) \rho_{\gamma\alpha} \rho_{\alpha\gamma'} \\ & + i \sum_\alpha (V_{\alpha\gamma}(t) \rho_{\alpha\gamma'} - V_{\gamma'\alpha}(t) \rho_{\gamma\alpha}) \end{aligned} \quad (6.50)$$

with  $U_\gamma$  defined as,

$$U_\alpha = \sum_{\beta} \lambda_{\alpha\beta} n_\beta. \quad (6.51)$$

If we assume that only states 1 and 2 are coupled and all the off-diagonal elements involving the other states are equal to zero, we get a very simple dynamics. The time derivative of the diagonal elements do not depend on  $\rho$ , while the off-diagonal element  $\rho_{12}$  changes according to

$$\begin{aligned} \dot{\rho}_{12} = & i \left( w_1 - w_2 + \sum_{\beta \neq 1,2} (\lambda_{\beta 1} - \lambda_{\beta 2}) n_\beta \right) \rho_{12} \\ & + i \sum_{\alpha} (V_{\alpha 1}(t) \rho_{\alpha 2} - V_{2\alpha}(t) \rho_{1\alpha}). \end{aligned} \quad (6.52)$$

When we go to the Bloch sphere representation in the basis rotating with the frequency of the external field, we have

$$\rho'_{\gamma\gamma'} = \rho_0 \delta_{\gamma\gamma'} + \vec{S}_f \cdot \vec{\sigma}_{\gamma\gamma'}, \quad (6.53)$$

and we get the simple equation of motion

$$\dot{\vec{S}}_f = 2\vec{S}_f \times \vec{V}. \quad (6.54)$$

which can be derived from the corresponding Hamiltonian,

$$\mathcal{H}_f = 2\vec{S}_f \cdot \vec{V}. \quad (6.55)$$

In the mean field picture, there are no coherent effects of interactions for a transition between the two states. The exchange contributions to the precession frequency exactly cancel the direct contributions. For short-range potentials, the exchange contribution to the energy has the same absolute value as the direct contribution. For Bosons, the two contributions add up, while for fermions they cancel.

The precession frequency for a free Fermi gas can be read off from Eq.(6.52),

$$\omega = (w_2 - w_1) + \sum_{\gamma \neq 1,2} (\lambda_{2\gamma} - \lambda_{1\gamma})n_{\gamma}. \quad (6.56)$$

This expression shows that the density dependent frequency shift encountered in the fountain atomic clocks can be eliminated, if a fermionic sample is used instead of a Bose gas. Any contributions to the frequency shift will be of higher order in the diluteness parameter  $a_s/(n^{-1/3})$  of the gas. Finally, we see that the behavior under an external field is not at all different from the usual Rabi precession. An analogue of internal Josephson effect does not appear since the “energy” of the system Eq.(6.55) does not depend on the density at all, that is, there are no quadratic terms in the Hamiltonian in the spin representation.

In conclusion, in this chapter we studied the effects of external interactions on the internal dynamics of atoms in a dilute gas, without making assumptions on the strength of the excitation. For a Bose gas, we first considered the general case of a partially condensed, non-uniform gas, and derived the transport equation. We then focused on the case of a homogeneous gas and investigated the effects of interactions on the internal degrees of freedom. As a first result, we obtained an expression for the density induced frequency shift in atomic clocks, for a gas which is above BEC temperature, or at zero temperature. Furthermore, we found that if a partially condensed sample is used in an atomic clock, one would get two density dependent frequencies instead of one, due to the exchange of atoms between the normal part and the condensed part of the gas. We then analyzed the effect of an external field. We showed how Rabi oscillations are replaced by internal Josephson oscillations as the strength of the external field is reduced. We calculated the frequencies of both oscillations exactly. We have also found that an analogue of the internal Josephson effect should be observable for a non-condensed sample.

Finally, we considered a Fermi gas, and derived the transport equation. We have found that it is possible to get rid of density caused frequency shifts by using a Fermi gas in an atomic clock, and that no analogue of internal Josephson effect is possible



for a Fermi gas.

# Chapter 7

## Conclusion

In this thesis, we studied the effects of interparticle interactions on the coherent internal state dynamics of a dilute system at low temperatures. We considered the case of weak excitation, in which the number of particles changing their internal state is negligible compared to the total number of particles. We derived an expression for the optical spectrum starting from the microscopic Hamiltonian of the system, and then used diagrammatic perturbation theory in the Random Phase Approximation to calculate the spectrum both above and below BEC.

We found that, for temperatures low enough to make the thermal de Broglie wavelength larger than the scattering length, exchange processes cause the optical excitations to become collective modes. Due to exchange, many particles are involved in the excitation process. We characterize this collective mode by the oscillation of the off-diagonal components of the density matrix. The collective nature of the excitation manifests itself in an interaction dependent dispersion relation for the optical mode, an extra shift for the average frequency of the spectrum, and in a line narrowing effect.

At lower temperatures, when BEC takes place, we found that the spectrum develops a doublet structure. One of the peaks is associated with the thermal component of the system, while the other is due to the condensate. We have then considered processes which mix those two modes, and calculated the resulting resonance frequencies for all temperatures below  $T_c$ .

We then derived an exact sum rule for the average frequency shift of the optical spectrum. We showed that the sum rule follows from some basic properties and symmetries of the system, and can be considered as an extension of the f-sum rule to systems with more than one internal state.

Finally, we relaxed the weak excitation assumption, and considered the non-linear optical response. We mapped the internal dynamics of the system to the evolution of two interacting anisotropic spins, and solved for their precession frequencies in various cases. This mapping allowed a comparison of the Rabi oscillations with the internal Josephson oscillations. We studied how the transition between them occurs when the external field strength is varied. Another important result obtained from this analysis is that, an analogue of the internal Josephson effect should be present for non-condensed cold gases. We also considered these effects for a Fermi system and found that the precession frequencies are affected by interactions only very weakly.

The research presented in this thesis was motivated by the observation of the optical spectrum of the spin polarized Hydrogen gas, above and below BEC. Although the presentation remained theoretical throughout, the resulting theory has some implications for existing experiments, and predicts some new effects. We conclude the thesis by giving a brief summary of these.

In the Hydrogen BEC experiments at MIT, optical spectroscopy was used as a tool to identify the condensation, by monitoring the large increase in density at the center of the trap. Thus, the phase transition was signaled not by the change in the optical spectrum per se, but by density change altering the optical spectrum. For homogeneous systems, however, condensation is not accompanied by any change in density. Consequently, it is somewhat harder to tell whether the system has actually undergone the phase transition. We have found that optical spectrum actually goes through a qualitative change upon condensation, even if there is no change in the density distribution. It has recently been suggested that this feature of our theory can be experimentally exploited to resolve the controversy over the BEC transition of excitons in  $\text{Cu}_2\text{O}$  [21].

The sensitivity of the optical spectrum upon interactions enables one to learn

more about how atoms interact with each other, through the measurement of optical properties. In particular, the sum rule derived in Chapter 5 can be very useful for measuring different scattering using the optical spectrum. If the measurement of the optical spectrum can be combined with an independent measurement of the density distribution, it should be possible to measure the scattering lengths very precisely.

Another class of experiments for which our results are relevant are those involving fountain atomic clocks. It is possible to use a partially condensed cloud of gas in a fountain atomic clock to study the properties of the condensed state. From our analysis that there will be two precession frequencies measured in such an experiment, which is distinctly different from what has been observed so far.

Besides that, a fountain atomic clock could be used to observe the internal Josephson effect in a BEC, and its analogue in a non-condensed cold gas. It would be interesting to explore experimentally the regime of switching between the Rabi oscillations and the internal Josephson oscillations. Finally, the dependence of the precession frequencies on density is a source of error in atomic clocks. It follows from our analysis that if fermions are used in these experiments, this density related shifts would be much smaller.

# Bibliography

- [1] A.A. Abrikosov, L.P. Gorkov, and I.E. Dyzalooshinskii. *Methods of Quantum Field Theory in Statistical Physics*, chapter 3. Prentice-Hall, Englewood Cliffs, New Jersey, 1963.
- [2] A.A. Abrikosov, L.P. Gorkov, and I.E. Dyzalooshinskii. *Methods of Quantum Field Theory in Statistical Physics*, chapter 5. Prentice-Hall, Englewood Cliffs, New Jersey, 1963.
- [3] A.A. Abrikosov, L.P. Gorkov, and I.E. Dyzalooshinskii. *Methods of Quantum Field Theory in Statistical Physics*, chapter 1. Prentice-Hall, Englewood Cliffs, New Jersey, 1963.
- [4] M. H. Anderson, J. R. Ensher, M. R. Matthews, C. E. Wieman, and E. A. Cornell. *Science*, 269:198, 1995.
- [5] G.B. Arfken and H.J. Weber. *Mathematical Methods for Physicists*, page 333. Academic Press, San Diego, 1995.
- [6] E.P. Bashkin. *JETP Letters*, 33:8, 1981.
- [7] E.P. Bashkin. *Soviet Physics JETP*, 60:1122, 1985.
- [8] S.T. Beliaev. *JETP*, 34:417, 1958.
- [9] C. C. Bradley, C. A. Sackett, J. J. Tollet, and R. G. Hulet. *Physical Review Letters*, 75:1687, 1995.

- [10] C. C. Bradley, C. A. Sackett, J. J. Tollet, and R. G. Hulet. *Physical Review Letters*, 78:985, 1997.
- [11] C. Cohen-Tannoudji, J. Dupont-Roc, and G. Grynberg. *Atom-Photon Interactions*, page 361. Wiley, New York, 1998.
- [12] K. B. Davis, M.-O. Mewes, M. R. Andrews, N. J. van Druten, D. S. Durfee, D. M. Kurn, and W. Ketterle. *Physical Review Letters*, 75:3969, 1995.
- [13] R.H. Dicke. *Physical Review*, 89:472, 1953.
- [14] D. G. Fried, T. C. Killian, L. Willmann, D. Landhuis, S. C. Moss, D. Kleppner, and T. J. Greytak. *Physical Review Letters*, 81:3811, 1998.
- [15] S. Ghezali, Ph. Laurent, S. N. Lea, and A. Clairon. *Europhysics Letters*, 36:25, 1996.
- [16] K. Gibble and S. Chu. *Physical Review Letters*, 70:1771, 1993.
- [17] I.S. Gradshteyn and I.M Ryzhik. *Table of Integrals, Series and Products*, page 228. Academic Press, San Diego, 1994.
- [18] D.S. Hall, M.R Matthews, J.R. Ensher, E.A. Cornell, and C.E. Wiemann. *Physical Review Letters*, 81:1539, 1998.
- [19] D.S. Hall, M.R. Matthews, C.E. Wiemann, and E.A. Cornell. *Physical Review Letters*, 81:1543, 1998.
- [20] K. Huang. *Statistical Physics*, chapter 5. John Wiley and Sons., New York, 1987.
- [21] K. Johnsen and G.M. Kavoulakis. *cond-mat/0006099*, 2000.
- [22] M.A. Kasevich, E. Riis, S. Chu, and R.G. DeVoe. *Physical Review Letters*, 63:612, 1989.
- [23] W. Ketterle. *Physica B*, 280:11, 2000.

- [24] T. C. Killian, D. G. Fried, L. Willmann, D. Landhuis, S. C. Moss, D. Kleppner, and T. J. Greytak. *Physical Review Letters*, 81:3807, 1998.
- [25] S.J.J.M.F. Kokkelmans, B.J. Verhaar, K. Gibble, and D.J. Heinzen. *Physical Review A*, 56:R4389, 1997.
- [26] R. Kubo. *Journal of Physical Society of Japan*, 12:570, 1957.
- [27] L.D. Landau and E.M. Lifshitz. *Quantum Mechanics*, volume 1, chapter 152. Butterworth Heinemann, Oxford, 1997.
- [28] L.D. Landau and E.M. Lifshitz. *Statistical Physics*, volume 1, chapter 7. Butterworth Heinemann, Oxford, 1997.
- [29] L.D. Landau and E.M. Lifshitz. *Statistical Physics*, volume 1, chapter 5. Butterworth Heinemann, Oxford, 1997.
- [30] R. Legere and K. Gibble. *Physical Review Letters*, 81:5780, 1998.
- [31] L.P. Lévy and A.E. Ruckenstein. *Physical Review Letters*, 52:1512, 1984.
- [32] C. Lhuillier and F. Laloë. *Journal of Physics (Paris)*, 43:197, 1982.
- [33] C. Lhuillier and F. Laloë. *Journal of Physics (Paris)*, 43:225, 1982.
- [34] E.M. Lifshitz and L.P. Pitaevskii. *Statistical Physics*, volume 2, chapter 3. Butterworth Heinemann, Oxford, 1995.
- [35] G.D. Mahan. *Many Particle Physics*, chapter 3. Plenum Press, New York, 1990.
- [36] G.D. Mahan. *Many Particle Physics*, chapter 7. Plenum Press, New York, 1990.
- [37] G.D. Mahan. *Many Particle Physics*, chapter 10. Plenum Press, New York, 1990.
- [38] P. Nozieres and D. Pines. *The Theory of Quantum Liquids*, volume 1, chapter 1. W.A. Benjamin, New York, 1966.
- [39] P. Nozieres and D. Pines. *The Theory of Quantum Liquids*, volume 1, chapter 2. W.A. Benjamin, New York, 1966.

- [40] P. Nozieres and D. Pines. *The Theory of Quantum Liquids*, volume 1, chapter 3. W.A. Benjamin, New York, 1966.
- [41] M.Ö. Oktel, T.C. Killian, D. Kleppner, and L.S. Levitov. *physics/9911020*, 1999.
- [42] M.Ö. Oktel and L.S. Levitov. *Physical Review Letters*, 83:6, 1999.
- [43] M. Pinard and F. Laloë. *Journal of Physics (Paris)*, 41:769, 1980.
- [44] M. Pinard and F. Laloë. *Journal of Physics (Paris)*, 41:799, 1980.
- [45] S. Raghavan, A. Smerzi, S. Fantoni, and S.R. Shenoy. *Physical Review A*, 59:620, 1999.
- [46] K. Sawada and et.al. In D.Pines, editor, *The Many Body Problem*, page 190. W.A. Benjamin, Inc., 1961.
- [47] E. Tiesinga, B. J. Verhaar, H. T. C. Stoof, and D. van Bragt. *Physical Review A*, 45:2671, 1992.
- [48] B. J. Verhaar, J. M. V. A. Koelman, H. T. C. Stoof, and O. J. Luiten. *Physical Review A*, 35:3825, 1987.
- [49] J. Weiner, V.S. Bagnato, S. Zilio, and P.S. Julienne. *Reviews of Modern Physics*, 71:1, 1999.
- [50] J. Williams, R. Walser, J. Cooper, E. Cornell, and M. Holland. *Physical Review A*, 59:R31, 1999.
- [51] I. Zapata, F. Sols, and A.J. Leggett. *Physical Review A*, 57, 1998.